1. Introduction

The Tohoku Earthquake on 11 March 2011 resulted in the release of large amounts of radioactive materials including iodine-131 (^{131}I) into the environment from the Fukushima Daiichi nuclear power plant. After the accident, ^{131}I was detected in drinking water in 15 out of the total 47 prefectures in Japan: the highest concentration in a village of Fukushima Prefecture was 1000 Bq/kg-water and the highest concentration in Tokyo Metropolitan was 200 Bq/kg-water (Ikemoto and Magara, 2011), which points to the importance of technologies for removal of radioactive substances during water purification processes. The radioactive iodine index levels for the restriction on drinking water intake in emergency by the Nuclear Safety Commission of Japan was 300 Bq/kg for the general public and 100 Bq/kg for infants (babies who take breast feeding or formula milk). The removal of radioactive iodine by 50–90 % was required.

The addition of powdered activated carbon (PAC) may be a feasible method for removal during conventional water treatment when accidents or incidents give rise to high levels of contamination in drinking water sources (Brown et al., 2008; Lettinga, 1972). However, the efficacy of ^{131}I removal by PAC was not sufficiently high. Kosaka et al. (2012) surveyed ^{131}I removal in water purification plants after the Fukushima accident and found that the removal percentages achieved by granular activated carbon and PAC were merely 30–40% or less. The authors also conducted laboratory tests and attained the removal efficiencies of 60–70% by PAC of the dosage 50 mg/L and the contact time 30 min after chlorination of the dosage 0.5–1 mg-Cl_2/L and reaction time 10 min.

Dissolved I (including ^{131}I) exists in various forms: molecular iodine (I_2), hypoiodite ion (IO^-), hypoiodous acid (HOI), iodide ion (I^-), iodate ion (IO_3^-), and organic iodine (organic-I). At neutral pH iodine can be present in the latter four forms (Bichsel and von Gunten, 2000a; Lettinga, 1972), while iodine is commonly found as I^-, IO_3^-, and organic-I in environmental waters (Davis et al., 2009; Gong and Zhang, 2013; Hansen et al., 2011). It has been reported that $^{131}I^-$ is poorly adsorbed by activated carbon (Ikeda and Tanaka, 1975; Lettinga, 1972). HOI is adsorbed on activated carbon to a greater extent than I^-: the adsorptive property of HOI is utilized in the iodine number, one of the most fundamental indicator widely used to characterize activated carbon as an adsorbent (AWWA, 1974). The removal of HOI is due to adsorption while that of chlorine is reductive reaction. Because HOI is formed by oxidation of I^-, the combination of chlorination and PAC adsorption could be effective for $^{131}I^-$ removal (Lettinga, 1972). However, $^{131}IO_3^-$, which is formed by oxidation of $HO^{131}I$, is reportedly not adsorbed by carbon (Lettinga, 1972). Therefore, chlorination of $^{131}I^-$ at a high chlorine dose, a long reaction time, or both would reduce the extent of adsorptive removal compared to that at a low dose and a short reaction time. During aqueous oxidation in the presence of natural organic matter (NOM), HOI reacts with NOM to form iodo-organic byproducts (Bichsel and von Gunten, 1999), which can be adsorbed by activated carbon (Summers et al., 1989). No systematic experimental study has been conducted to clarify how chlorination time, carbon type, and carbon dose affect iodine species distribution and, thus, iodine removal efficacy.

In this study, we systematically investigated the formation of iodine species by chlorination and their removal from water by activated carbon adsorption. The effects of chlorine dose, chlorination time, carbon particle size, NOM content, and co-existing bromide on iodine removal were evaluated to determine the optimum conditions for removal of radioactive iodine from water. We used ^{127}I rather than ^{131}I. But the adsorption behavior of ^{127}I is similar to that of ^{131}I. Therefore, information regarding ^{127}I removal can be expected to provide important insights for the removal of ^{131}I. The removal of iodide in water is also of great significance for controlling the formation of iodinated disinfection byproducts (Ding and Zhang, 2009; Plewa et al., 2004). Hereafter, we refer to ^{127}I simply as I (or iodine).

2. Materials and methods

2.1. Sample water

NOM-free water was prepared by adding inorganic ions to ultrapure water (Milli-Q Advantage, Millipore) so that the ionic composition was equal to that of water from Lake Hakucho, Hokkaido, Japan (Table S1, Supplementary Material) (Ando et al., 2010). NOM water was prepared by adding Suwannee River NOM (International Humic Substance Society) to the NOM-free water to bring the dissolved organic carbon (DOC) concentration to 1.5 mg-C/L unless otherwise noted. Potassium iodide was added to the NOM-free water and the NOM water, and then the pH was adjusted to 7.0 with HCl or NaOH; the iodine concentration was 10 μg-I/L, which is typical of natural surface waters. In the experiments on iodine removal in the presence of bromide ion (Br^-), KBr was also added, at concentrations ranging from 0 to 2000 μg-Br/L (Jones et al., 2011; Richardson et al., 2008). All chemicals used were regent grade (Wako Pure Chemical, Osaka, Japan).

2.2. Activated carbon

Two types of activated carbon were used. A commercially available, thermally activated wood-based PAC (median particle diameter, 18.9 μm) was obtained from Taiko-W, Futamura Chemical (Nagoya, Japan). A superfine PAC (SPAC, median particle diameter, 0.62 μm; Figures S1 and S2, Supplementary Material) was prepared by microgrinding the PAC with a bead mill (Metawater, Tokyo) (Ando et al., 2010). PAC and SPAC were stored as slurries in ultrapure water at 4 °C and used after dilution. The particle size distributions of PAC and SPAC were determined with a laser-light scattering instrument (Microtrac MT3300EXII, Nikkiso, Tokyo) following the addition of a dispersant (Triton X-100, Kanto Chemical, Tokyo; final concentration, 0.08 vol%) and ultrasonication.

2.3. Batch oxidation and adsorption tests

Sample water was treated with chlorine (in the form of sodium hypochlorite, Wako Pure Chemical) at concentrations of 0.01–50 mg-Cl_2/L for 1–60 min, and then activated carbon was added. After a carbon contact time of up to 30 min, the

suspension was filtered through a 0.2-μm membrane filter (DISMIC-25HP; Toyo Roshi Kaisha, Tokyo). In some experiments, water was treated first with carbon and then with chlorine. All experiments were conducted in the room temperature of 20 °C. Individual operation condition is described in figures. The concentration of free chlorine was determined by means of the *N,N*-diethyl-*p*-phenylenediamine colorimetric method (DR/4000U, Hach).

2.4. *Iodine fractionation*

The total iodine concentrations in sample waters were determined by means of inductively coupled plasma mass spectrometry (ICP-MS; 7700 series, Agilent Technologies) with tellurium as an internal standard (detection limit: 0.2 μg-I/L). Iodine fractionation was conducted by using total organic halide (TOX) analysis and ion-chromatography with post-column (IC-PC) derivatization (ICS-1100, PCM 520, UVD-510, Dionex) both for the samples treated with and without chlorine (Figures S3, Supplementary Material). The IC-PC was conducted according to the Dionex manual. KaBr/$NaNO_2$ mixture was used as PC derivatization reagent in order to form tri-iodide, which is detected using UV detector at 268 nm (detection limit: 0.1 μg-I/L).

Water samples with/without 10-min chlorination were treated with SPAC at a concentration of 100 mg/L for 30 min (these condition were determined for the complete removal of adsorbable iodine and bromine) and then filtered through a 0.2-μm PTFE membrane filter to obtain Sample A, which contained I^- and IO_3^- but did not contain HOI, as indicated by the results of a preliminary experiment (Supplementary Material, Section 1 and Figure S4). The total iodine concentration in Sample A was determined by ICP-MS, the IO_3^- concentration was determined for Sample A by IC-PC, and the I^- concentration was calculated for Sample A by subtracting the IO_3^- concentration from the total iodine concentration.

The organic-I concentrations were measured by means of TOX analysis, as follows (see Supplementary Material, Section 2 for details). After chlorination, NOM water was applied to a column of activated carbon. Then the column was washed with KNO_3 solution to remove any HOI bound to the carbon. The carbon packing was then removed from the column and heated in a muffle furnace, and the combustion gas was bubbled through Milli-Q water (the resulting solution was designated as Sample B). Any iodine in Sample B was regarded as organic-I (Tate et al., 1986). The iodine concentration in Sample B was determined by means of ICP-MS. The concentration of HOI was calculated by subtracting the iodine concentrations in Samples A and B from the initial iodine concentration, which was determined by ICP-MS. The percentages obtained by the fractionation method were verified by comparing them with the concentrations obtained by an alternative method (Supplementary Material, Section 3 and Figure S5) in which the concentration of HOI in the eluent from the activated carbon column used for TOX analysis was determined by ICP-MS.

2.5. *Bromine fractionation*

Bromine was fractionated in conjunction with iodine fractionation. The total bromine concentration and the bromate ion (BrO_3^-) concentration were determined by ICP-MS (detection limit: 5 μg-Br/L) and IC-PC (detection limit: 0.5 μg-Br/L), respectively (Figures S6, Supplementary Material). Because Br^- is not adsorbed by activated carbon whereas hypobromous acid (HOBr), BrO_3^-, and organic bromine (organic-Br) are adsorbed (Siddiqui et al., 1996), the concentration of Br^- was determined by means of ICP-MS for Sample A (the mechanism that HOBr is adsorbed but not reduced to Br^- by activated carbon was confirmed by the decrease of total bromine concentration determined by ICP-MS. Section 3.3). The organic-Br concentration was measured for Sample B by means of ICP-MS. The HOBr concentration was calculated by subtracting the sum of the concentrations of Br^-, BrO_3^-, and organic-Br from the total bromine concentration.

2.6. *Direct observation of iodine adsorbed on PAC particles*

To obtain PAC particles containing adsorbed HOI and adsorbed organic-I, we conducted batch adsorption experiments. After batch adsorption, PAC particles were removed, placed on a silicon wafer, and then cut. Iodine adsorbed on the cut PAC particles was directly observed by means of scanning electron microscopy and field emission electron probe microanalysis (FE-EPMA; JXA-8530F, JEOL). Details of these experiments are described in the Supplementary Material (Section 4 and Figures S7 and S8).

3. Results and discussion

3.1. *Iodine removal by activated carbon after chlorination*

Without prior chlorination, I^- in the NOM-free water was not removed by activated carbon treatment (Figure S9, Supplementary Material). No removal of I^- from NOM water was observed either. In contrast, when chlorine was added to the NOM-free water before activated carbon treatment, about 40% of the iodine was removed. After the chlorination, iodine in the NOM water was removed at a higher percentage (90%) by activated carbon treatment than in the NOM-free water. This removal percentage was similar but slightly higher than the DOC removal percentage (80%). The similar removal suggests that the formation of organic-I was responsible for the high iodine removal percentage in the presence of NOM. The slightly higher removal is possibly due to HOI removal.

We further studied the effect of NOM by varying the initial DOC concentration in the sample water. Even a DOC concentration as low as 0.5 mg-C/L drastically improved adsorptive removal of iodine by SPAC after chlorination (Panel A of Fig. 1). At a fixed SPAC dose of 100 mg/L, the residual iodine ratio decreased as the initial DOC concentration was increased from 0 to 3 mg-C/L, but the ratio increased as the DOC concentration was increased further from 3 to 10 mg-C/L. This increase in residual ratio was due to the insufficiency of the carbon dose; when the carbon dose was increased to >100 mg/L, the ratio continued to decrease with increasing DOC concentration above 3 mg-C/L (Fig. 1, Panel A, dashed line). The residual ratios indicated by the triangles in Panel A

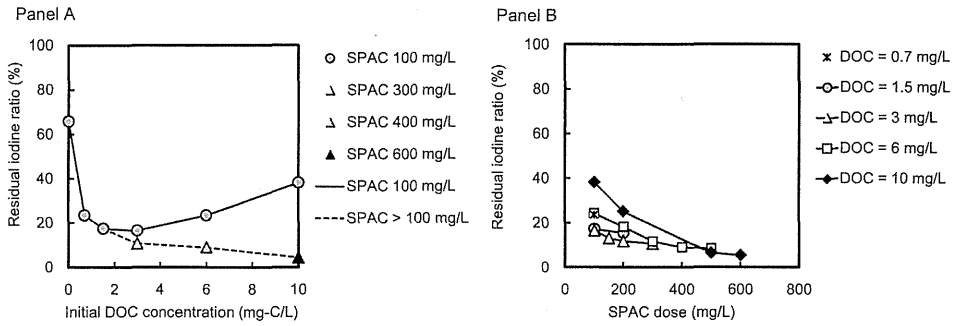

Fig. 1 – Effect of initial DOC concentration (left) and SPAC dose (right) on iodine removal from NOM water by chlorination followed by treatment with SPAC. Initial I^- concentration in sample water, 10 μg-I/L; chlorine dose, 1 mg-Cl_2/L; chlorination time, 10 min; carbon contact time, 30 min.

of Fig. 1 were achieved when a sufficient amount of SPAC was used; the amount that was sufficient was confirmed by testing various combinations of SPAC dose and DOC concentration (Fig. 1, Panel B). The data points indicated by the triangles can be considered to be the lowest residual iodine ratios attainable by adsorptive removal with SPAC. These results indicate that the percentage of iodine converted to adsorbable forms increased with increasing NOM concentration: at the DOC of 10 mg-C/L, 95% of I^- was converted to adsorbable forms.

3.2. *Chlorine-dose dependence and iodine fractionation analysis*

The results described in the previous section indicate that the iodine was converted to an adsorbable form by chlorination. Next we studied the effect of chlorine dose. For NOM-free water, a chlorine dose of approximately 0.1 mg-Cl_2/L was found to be optimal, yielding the lowest residual iodine ratio (Figure S10, Supplementary Material). A similar trend was observed for NOM water, although low residual iodine ratios were observed over a broader range of chlorine doses (0.1–1.0 mg-Cl_2/L). Iodine removal increased with increasing chlorine dose up to 0.1 mg-Cl_2/L but decreased at chlorine doses of >1.0 mg-Cl_2/L. Overall, the residual ratios were lower in the presence of NOM than in its absence.

To elucidate the mechanism of the dependence of iodine removal on chlorine dose, we conducted iodine fractionation. In NOM-free water (Fig. 2, Panel A), the production of HOI was highest at a chlorine dose of 0.05–0.1 mg-Cl_2/L, and production decreased as the chlorine dose was increased from 0.1 to 10 mg-Cl_2/L. Therefore, a moderate chlorine dose (0.05–0.1 mg-Cl_2/L) was most effective for the formation of HOI, which was adsorbed by activated carbon. At high chlorine doses (>0.1 mg-Cl_2/L), IO_3^- formed, and IO_3^- became the major species at chlorine doses of >1 mg-Cl_2/L. The percentages of IO_3^- fraction were almost similar but somewhat higher than those calculated by the reaction rate constants reported previously (Bichsel and von Gunten, 1999): the experimental percentages were 1.9, 38, and 100 while the calculated ones were 1.5, 14, and 88 at the chlorine doses of 0.1, 1 and 10 mg-Cl_2/L, respectively. The somewhat higher IO_3^- percentages might be due to the enhanced oxidation at very low iodine concentration in our experiments.

When the water contained NOM (DOC concentration, 1.5 mg-C/L), organic-I formed (Fig. 2, Panel B). The concentration of organic-I increased as the chlorine dose was

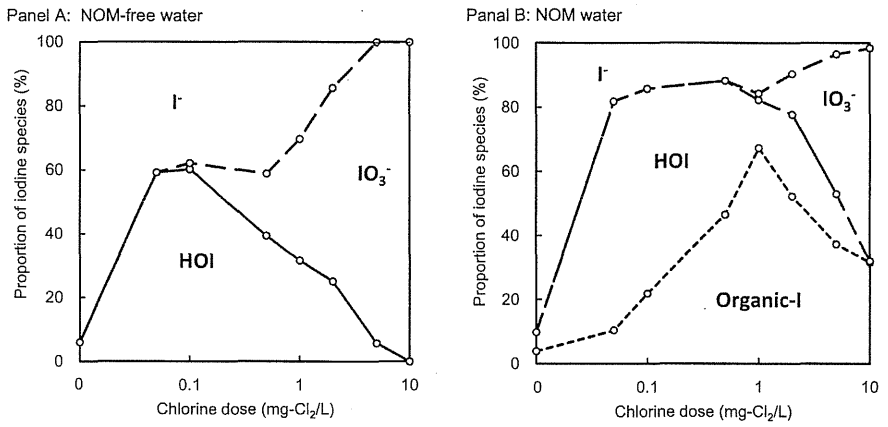

Fig. 2 – Proportions of iodine species in NOM-free water (left) and NOM water (right) as a function of chlorine dose. Chlorination time, 10 min; initial I^- concentration in sample water, 10 μg-I/L; initial DOC concentration in NOM water, 1.5 mg-C/L.

increased from 0.05 to 1 mg-Cl_2/L, and then it decreased. The latter finding is qualitatively in agreement with the results of studies of iodotrihalomethane formation, in which an increase in chlorine doses was found to lead to a decrease in the levels of iodinated organic byproducts and an increase in IO_3^- formation (Bichsel and von Gunten, 2000b; Hua et al., 2006). We found that organic-I was the major species at high chlorine doses (0.5–5 mg-Cl_2/L) and that HOI was the major species at low doses (0.05–0.5 mg-Cl_2/L). We inferred that at chlorine doses of >1.0 mg-Cl_2/L in the NOM-free water, HOI was promptly oxidized to IO_3^-, which was not adsorbed by activated carbon. However, in the NOM water at a high chlorine dose, the formation of organic-I prevented the formation of IO_3^-. The use of chlorine doses of 0.1–0.5 mg-Cl_2/L resulted in the formation of the highest amount of adsorbable iodine (HOI and organic-I) and thus to the highest iodine removal efficiency.

3.3. *Effect of co-existing Br^- on the removal of I^-*

Br^- have been shown to influence the formation of iodinated trihalomethane during water treatment by means of chlorination (Jones et al., 2012), and thus the presence of Br^- can be expected to have an impact on iodine oxidation by chlorination. As shown in Panel A of Fig. 3, the residual iodine ratio in the NOM-free water slightly increased as the Br^- concentration was increased from 0 to 10 μg-Br/L, and the increase in residual iodine ratio with increasing Br^- concentration was more rapid in the concentration range from 10 to 200 μg-Br/L. This result indicates that co-existing Br^- in the water inhibited iodine removal. In the NOM-free water, IO_3^- formation increased dramatically with increasing initial Br^- concentration in the range from 10 to 200 μg/L (Panel B of Fig. 3). In contrast, little IO_3^- was formed in the presence of Br^- in the NOM water. The effect of Br^- on iodine removal was largely attributable to enhanced formation of nonadsorbable IO_3^- in the presence of Br^-.

To further elucidate the effect of Br^- on the oxidation of I^- by chlorine, we conducted iodine and bromine fractionation. As shown in Panel A1 of Fig. 4, in NOM-free water containing Br^-, the proportion of HOI was the largest at a chlorine dose of 0.1 mg-Cl_2/L. IO_3^- formed at chlorine doses of >0.1 mg-Cl_2/L and became the major iodine species at chlorine doses of >1 mg-Cl_2/L. This result was similar to that observed in the absence of Br^- (Fig. 2, Panel A). However, the percentage of IO_3^- formation at chlorine doses of >0.1 mg-Cl_2/L (and particularly at a chlorine dose of ~1 mg-Cl_2/L) was higher in the presence of Br^- than in the absence of Br^-. At a chlorine dose of 1 mg-Cl_2/L, IO_3^- formation in the presence of Br^- was 1.7 times that in the absence of Br^-. Bromine fractionation revealed that in the NOM-free water, HOBr was formed at a chlorine dose of 0.05 mg-Cl_2/L, and the proportion of HOBr increased with increasing chlorine dose up to 2 mg-Cl_2/L (Fig. 4, Panel B1). This chlorine dose range roughly coincided with the range at which IO_3^- formation was higher in the presence of Br^- than in its absence. It was recently reported that increasing the Br^- concentration increases the oxidation of HOI to IO_3^- (Criquet et al., 2012), as a result of a bromide-catalyzed process where the following reaction sequence is proposed. HOBr is formed through the reaction of chlorine with Br^-. HOBr then oxidizes HOI to IO_3^- and thereby HOBr is reduced to Br^-. Our results confirm that Br^-/HOBr-catalyzed process: we found that when HOBr was formed by the oxidation of Br^- by chlorine, the oxidation of HOI to IO_3^- was enhanced.

In the NOM water, iodine removal was not greatly influenced by the presence of Br^- (Panel A of Fig. 3). However, the nature of the adsorbed iodine species differed in the absence and presence of Br^- (Fig. 2, Panel B; Fig. 4, Panel A2). More organic-I was formed at a chlorine dose of ~0.1 mg/L in the presence of Br^- than in its absence, while more IO_3^- was formed at chlorine doses >5 mg/L. The enhanced formation of organic-I may possibly be due to a reaction process similar to the Br^-/HOBr-catalyzed process of IO_3^- formation. As shown in panel B2 of Fig. 4, the proportion of HOBr was high at chlorine doses of >0.5 mg-Cl_2/L. However, at chlorine doses ranging from 0.05 to 0.1 mg-Cl_2/L, the proportion of HOBr was low. Nonetheless, a large amount of organic-I was formed at this low chlorine dose range. There is, however, a possibility that

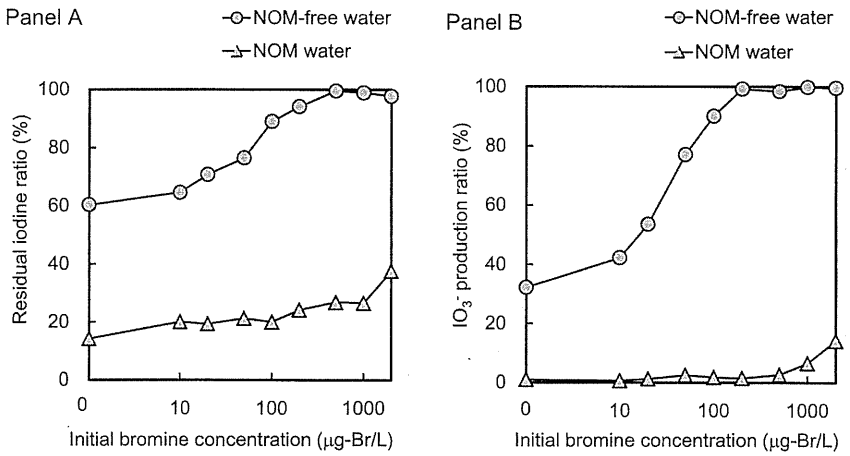

Fig. 3 – Effect of initial Br^- concentration on adsorptive removal of iodine (left) and IO_3^- production ratio (right). SPAC dose, 100 mg/L; initial I^- concentration in sample water, 10 μg-I/L; initial DOC concentration in NOM water, 1.5 mg-C/L; chlorine dose, 1.0 mg-Cl_2/L; chlorination time, 10 min; carbon contact time, 30 min.

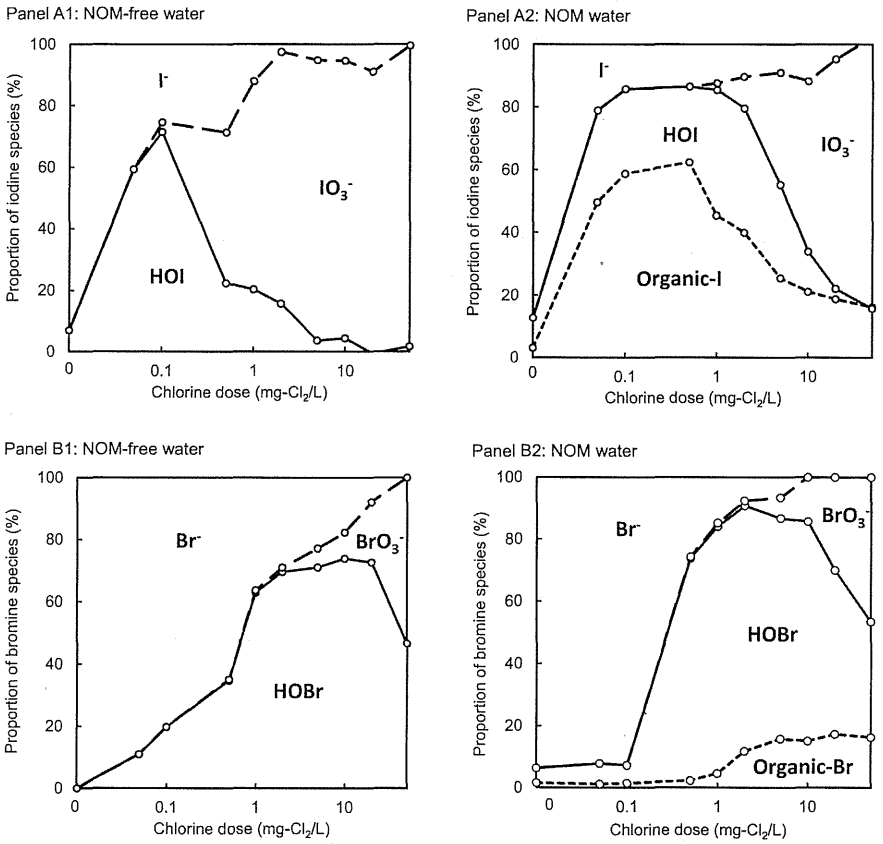

Fig. 4 – Proportions of iodine species (top) and bromine species (bottom) formed in the presence of Br^- as a function of chlorine dose. Chlorination time, 10 min; initial I^- concentration in sample water, 10 μg-I/L; initial Br^- concentration, 100 μg-Br/L; initial DOC concentration in NOM water, 1.5 mg-C/L.

HOBr had been once formed but it was converted back to Br^-. Without clear data of HOBr formation, it cannot be concluded that organic-I was formed through the Br–/HOBr-catalyzed process. Further study is granted for the mechanism of the enhanced formation of organic-I in the presence of bromide.

3.4. *Effects of chlorination and reaction sequence*

We also evaluated the effect of chlorination time (1–60 min) on the residual iodine ratio (Fig. 5). The lowest residual ratio was observed at the shortest chlorination time (1 min). This result suggests that the oxidation of I^- to HOI was fast and that the oxidation of HOI to IO_3^- occurred continuously as long as free chlorine was present in the water. The fast oxidation reaction of I^- to HOI and the following slow oxidation reaction of HOI to IO_3^- are in agreement with the reaction kinetics calculations with the rate constants reported previously (Bichsel and von Gunten, 1999; Criquet et al., 2012; Kumar et al., 1986): half life of I^- in the presence of HOCl of >1 mg-Cl_2/L is < 1 ms while that of HOI was <45 min. Therefore

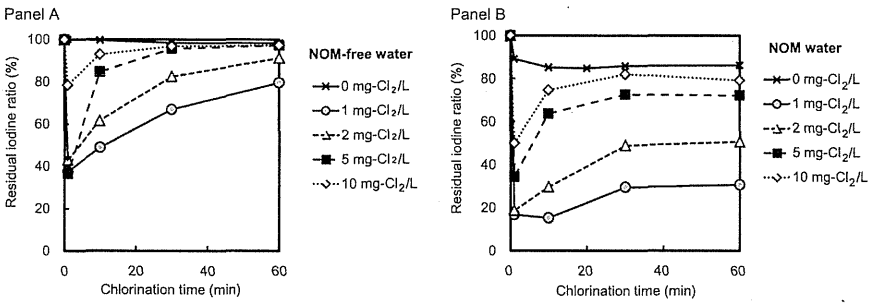

Fig. 5 – Effects of chlorination time and chlorine dose on iodine removal from NOM-free water (left) and NOM water (right). After chlorination, 100 mg/L of SPAC was added. Initial I^- concentration in sample water, 10 μg-I/L; initial DOC concentration in NOM water, 1.5 mg-C/L; carbon contact time, 30 min.

chlorination in the presence of carbon could enhance iodine removal if HOI adsorption occurred before HOI was oxidized to IO_3^-. To evaluate this possibility, we conducted two experiments: in one experiment (Case 1), water was chlorinated first and then activated carbon was added, whereas in the other experiment (Case 2), water was chlorinated after activated carbon was added.

In the NOM-free water (Fig. 6, panel A1), lower residual iodine ratios were obtained in Case 2 than in Case 1 at chlorine doses of >0.3 mg-Cl_2/L. Panel A2 of Fig. 6 shows IO_3^- formation ratio and residual chlorine ratios for the two experiments. In Case 2, the formation of IO_3^- was depressed compared to that in Case 1. The carbon consumed the chlorine so that the formation of IO_3^- by oxidation of HOI was suppressed. Therefore, after HOI formed, it was efficiently adsorbed by the carbon. At low chlorine doses (<0.2 mg-Cl_2/L), however, iodine removal was lower in Case 2 than in Case 1, owing to the consumption of chlorine by carbon before the chlorine could oxidize I^- to HOI.

We also compared the results for Cases 1 and 2 with NOM water. Although iodine removal was higher in Case 2 than in Case 1 at high chlorine doses (>5 mg-Cl_2/L; Fig. 6, panel B1), the difference between the two cases for the NOM water was not as clear as that for the NOM-free water. This result is reasonable because IO_3^- formation in the NOM water was depressed by the formation of organic-I, even in the absence of activated carbon; the IO_3^- formation was smaller in the presence of NOM than in the absence of NOM (compare Panels B2 and A2 of Fig. 6). The formation of IO_3^- was also somewhat depressed when the water was treated with activated carbon prior to chlorination (Case 2), and consequently iodine removal was slightly higher in Case 2 than in Case 1.

In Case 1, increasing the chlorine contact time depressed adsorptive removal of iodine because of the formation of IO_3^- from HOI (Fig. 5). However, a similar trend was not observed in Case 2, as shown in panels A1 and B1 of Fig. 7. The residual iodine ratios did not increase with increasing chlorine contact time; instead, the removal percentage increased until 10 min. This result also supports the reaction mechanism described above: soon after I^- was oxidized to HOI by chlorine, the HOI was adsorbed by the carbon, and only some of the HOI was further oxidized to IO_3^- in the presence of carbon. Meanwhile, activated carbon consumed the chlorine, which disappeared after 10 min (Fig. 7, panels A2 and B2). Therefore, iodine removal did not increase; rather, it reached a constant level after 10 min.

3.5. *Effect of carbon particle size on adsorption capacity*

The effect of carbon particle size on adsorption capacity was examined by calculating the adsorption isotherms from data obtained by batch adsorption experiments on prechlorinated sample water containing iodine. In the batch adsorption experiments, the water-phase iodine concentration did not change when the contact time was increased from 30 to 60 min (Figure S11, Supplementary Material). Therefore, we assumed that adsorption equilibrium was attained at a contact time of 30 min. The adsorption isotherms (Fig. 8) were obtained by mass balance after contact with PAC or SPAC, but note that the iodine in the water-phase might have consisted

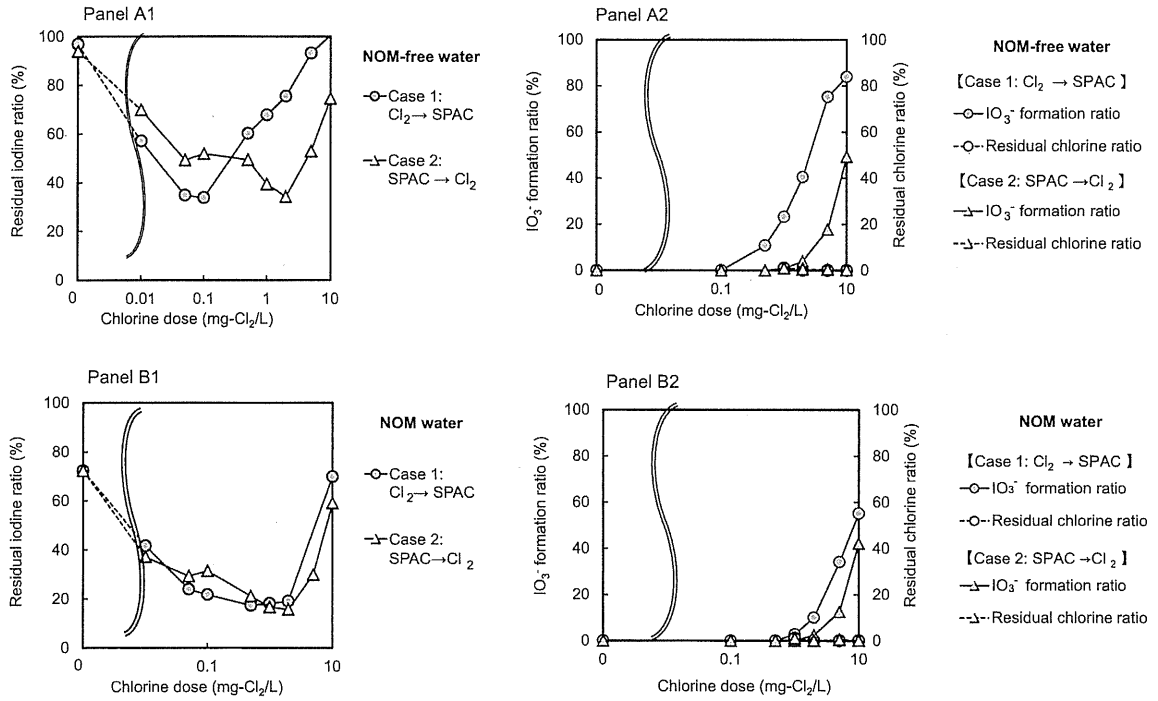

Fig. 6 – Effects of reaction sequence on residual iodine ratios (left) and IO_3^- formation ratios (right) in NOM-free water (top) and NOM water (bottom). Case 1: Chlorination followed by activated carbon treatment. Case 2: Chlorination preceded by activated carbon treatment. Initial I^- concentration in NOM water, 10 μg-I/L; SPAC dose, 100 mg/L; chlorination time, 10 min; carbon contact time for Case 1, 30 min; initial DOC concentration in NOM water, 1.5 mg-C/L.

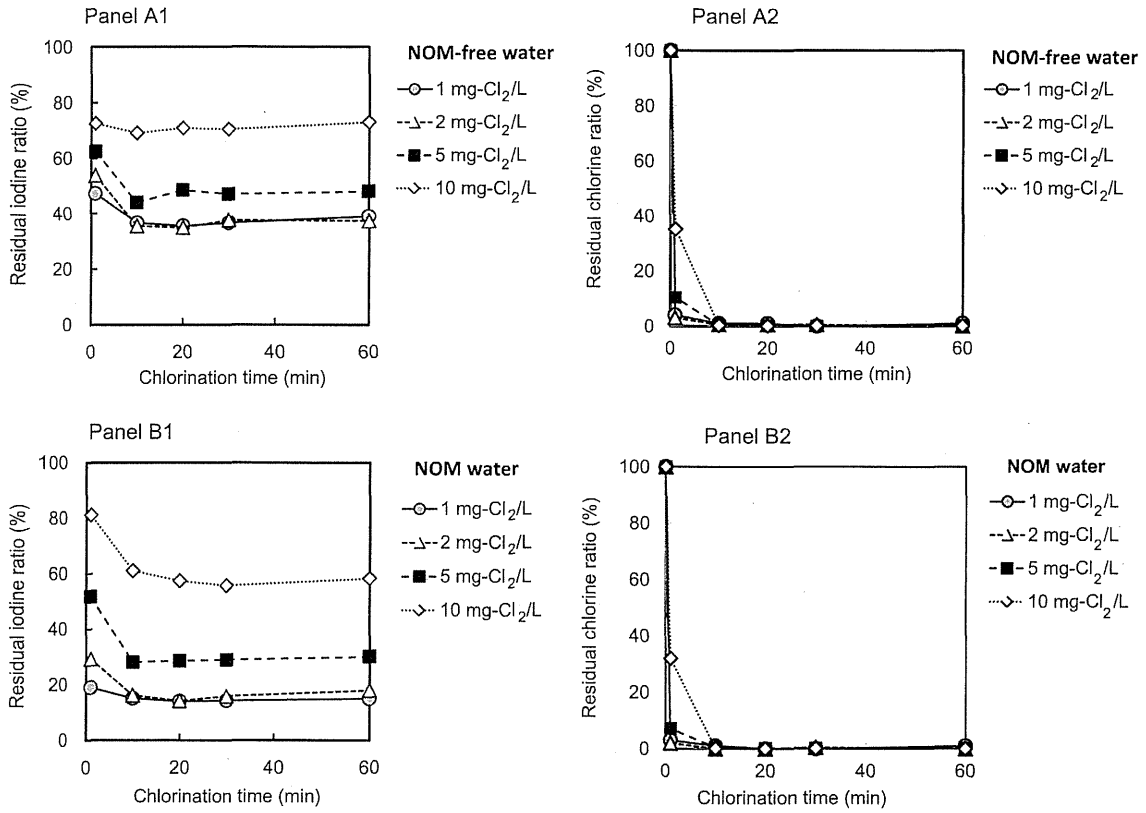

Fig. 7 – Effects of chlorination time and chlorine dose on residual iodine ratio (left) and residual chlorine ratio (right) in NOM-free water (top) and NOM water (bottom). After SPAC was added to the sample water, chlorine was added. SPAC dose, 100 mg/L; initial I^- concentration in sample water, 10 μg-I/L; initial DOC concentration, 1.5 mg-C/L.

of both adsorbable iodine (HOI and/or organic-I) and non-adsorbable iodine (I^- and IO_3^-). At a given water-phase iodine concentration (x-axis of Fig. 8), which was attained by one removal percentage, the adsorbable iodine (HOI and/or organic-I) concentrations were the same between SPAC and PAC because the prechlorination conditions were the same for the water samples. Therefore, the adsorption capacities of PAC and SPAC can be compared at a given water-phase concentration in Fig. 8. The adsorption isotherms for SPAC and PAC were the same for the NOM-free water (Fig. 8, Panel A), whereas the isotherms were different for the NOM water (Fig. 8, Panel B). In the presence of NOM, the adsorption capacity of PAC was roughly half that of SPAC. Such a trend of the lower adsorption capacity of PAC than of SPAC is reported for NOM adsorption (Ando et al., 2010), and the low adsorption capacity of PAC compared with that of SPAC is due to the difference in carbon particle size and to external adsorption: adsorbates do not diffuse into the interior of the PAC particles and instead are preferentially adsorbed near the particle surface (Ando et al., 2011; Matsui et al., 2011). Therefore, not all of the internal pore surface of the PAC particles is used for adsorption. In contrast, adsorbates can completely penetrate SPAC particles because the radial diffusion distance is short, and thus the entire internal pore surface of the SPAC particles is used for adsorption. The fact that there was no difference in adsorption capacity between PAC and SPAC for the NOM-free water indicates that internal adsorption occurred for both PAC and SPAC. Therefore, the experimental results for the NOM-free water indicate that HOI was adsorbed on the internal pore surface of the PAC particles. The experimental results for the NOM water indicate that organic-I was adsorbed on the external surface of the PAC particles. This is reasonable if the adsorption characteristics of organic-I (or iodinated NOM) are similar to those of the parent NOM, which exhibits external adsorption (Ando et al., 2010).

3.6. *Visualization of solid-phase iodine concentration profiles*

To verify the internal adsorption of HOI and the external adsorption of organic-I on PAC particles, we visualized the solid-phase iodine concentration profiles by using FE-EPMA. Panels A3 and A4 of Fig. 9 are iodine intensity maps of a cut PAC particle containing adsorbed HOI formed by chlorination in the NOM-free water. The intensity from iodine was slightly lower outside the particle (~230 cps) than inside the particle (~270 cps). However, this difference may have been due to the edge effect: the intensity from carbon was also slightly lower outside than inside (Fig. 9, Panel A2). An area of low intensity was also observed at the center right of the sample. However,

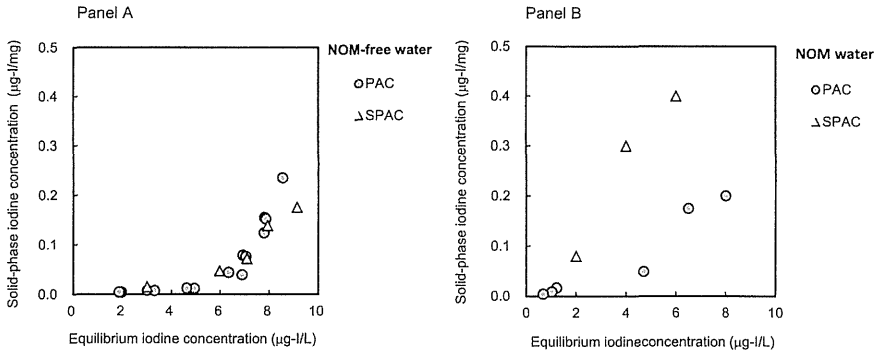

Fig. 8 – Comparison of iodine adsorption isotherms for PAC and SPAC in NOM-free water (left) and NOM water (right). After chlorination of sample water for 10 min, PAC or SPAC was added. Initial I^- concentration in sample water (NOM water and NOM-free water), 10 μg-I/L; chlorine doses, 0.5 mg-Cl_2/L for NOM-free water and 1.0 mg-Cl_2/L for NOM water; initial DOC concentration in NOM water, 1.5 mg-C/L; carbon contact time, 30 min.

there was a large open pore at the center right (Fig. 9, Pane A1), and thus the low intensity at the center right does not indicate low iodine concentration. Therefore, this result suggests that HOI was adsorbed uniformly in the PAC particle.

Iodine intensity maps of a cut sample of a PAC particle containing adsorbed organic-I formed by chlorination in the NOM water are shown in panels B3 and B4 of Fig. 9 (both HOI and organic-I were formed in the NOM water, but the HOI was eluted from the carbon particle, as described in the Supplementary Material, Section 3). For this particle, the iodine intensity was not higher inside than outside; instead the intensity was lower inside (~110 cps) than outside (~160 cps). Four open pores were observed in the sample (Fig. 9, panel B1). Therefore, the low intensity in the area close to these pores may have been due to the pores. However, there was a large area of low intensity (the area surrounded by the dotted line in Fig. 9) away from these pores. This result indicates that the concentration of solid-phase organic-I was lower inside the carbon particle than outside and that organic-I was adsorbed more on the outside than on the inside.

Overall, the visualization verified the hypothesis described in the previous section (external adsorption of organic-I and internal adsorption of HOI). The organic-I was adsorbed on the surface region of the PAC particles, but the total external surface area per unit weight of carbon was increased by the pulverization of PAC to SPAC. Accordingly, the increase in the surface area gave an advantage to SPAC compared to PAC with respect to organic-I adsorption capacity.

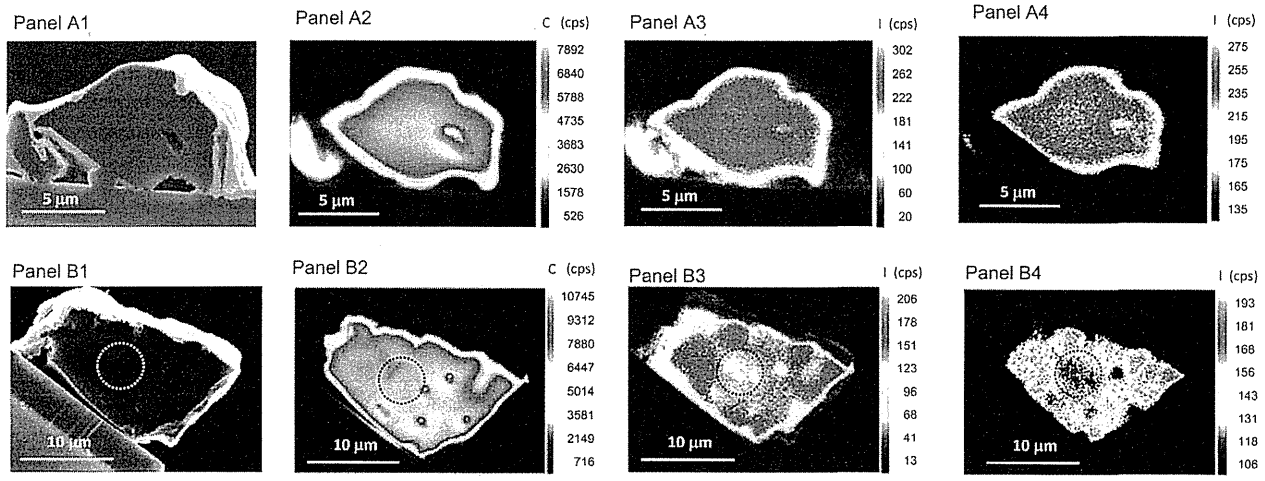

Fig. 9 – Surface elemental analysis of cut PAC particles with adsorbed HOI (A1–A4) and adsorbed organic-I (B1–B4) by means of field emission electron probe microanalysis (FE-EPMA). Initial I^- concentration in sample water, 10,000 μg-I/L; initial DOC concentrations, 0 mg-C/L for panels A1–A4 and 1.5 mg-C/L for panels B1–B4. After chlorination for 10 min at 5 mg-Cl_2/L, PAC was added. After a carbon contact time of 30 min, PAC particles were removed and cut with a focused ion beam. (A1) Scanning electron micrograph of a cut PAC particle, (A2) elemental mapping of carbon (C) (526–7892 cps), (A3) elemental mapping of iodine (I) (0–323 cps), and (A4) elemental mapping of iodine (I) (125–285 cps). (B1) Scanning electron micrograph of a cut PAC particle, (B2) elemental mapping of carbon (C) (716–10,745 cps), (B3) elemental mapping of iodine (I) (0–220 cps), (B4) elemental mapping of iodine (I) (100–200 cps).

4. Conclusions

(1) HOI and organic-I were adsorbed by activated carbon. In the presence of NOM, HOI was the major adsorbed species at a low chlorine dose, whereas organic-I was the major species at a high chlorine dose.
(2) There was an optimum chlorine dose for transformation of iodine to its adsorbable forms. The optimum dose was relatively low: 0.5–1.0 mg-Cl_2/L for 10 μg/L of iodine in the presence of NOM (1.5 mg-DOC/L). A long chlorination time reduced iodine removal because of the transformation of HOI to nonadsorbable IO_3^-. The optimum chlorination time was ~1 min or less.
(3) In the presence of Br^- in the NOM-free water, I^- was easily transformed into IO_3^- by chlorination even at low chlorine doses (0.1–0.2 mg-Cl_2/L), owing to a Br^-/HOBr-catalyzed process; and this process resulted in lower iodine removal in the presence of Br^- than in its absence. In the NOM water, however, co-existing Br^- did not decrease iodine removal greatly, owing to the high production of organic-I.
(4) In the NOM-free water, chlorination in the presence of PAC (Case 2) could enhance iodine removal compared with prechlorination followed by PAC adsorption (Case 1). This difference was due to the fact that in Case 2, the formation of IO_3^- was minimized by the consumption of chlorine by carbon. After HOI formed, it was readily adsorbed by the activated carbon before it could be oxidized to IO_3^-. In the NOM water, however, iodine removal was similar in Cases 1 and 2.
(5) The HOI adsorption capacity of SPAC was similar to that of PAC. For organic-I, however, SPAC showed higher adsorption capacity than PAC, because of the external adsorption (organic-I was adsorbed close to the PAC particle surface).
(6) FE-EPMA of PAC particles containing adsorbed HOI and organic-I revealed that the organic-I was adsorbed mostly close to the external surface of the PAC particles, whereas HOI was adsorbed uniformly in the PAC particles.

Acknowledgments

This study was supported by a Grant-in-Aid for Scientific Research S (no. 24226012) from the Japan Society for the Promotion of Science.

Appendix A. Supplementary data

Supplementary data related to this article can be found at http://dx.doi.org/10.1016/j.watres.2014.10.021.

REFERENCES

Ando, N., Matsui, Y., Kurotobi, R., Nakano, Y., Matsushita, T., Ohno, K., 2010. Comparison of natural organic matter adsorption capacities of super-powdered activated carbon and powdered activated carbon. Water Res. 44 (14), 4127–4136.

Ando, N., Matsui, Y., Matsushita, T., Ohno, K., 2011. Direct observation of solid-phase adsorbate concentration profile in powdered activated carbon particle to elucidate mechanism of high adsorption capacity on super-powdered activated carbon. Water Res. 45 (2), 761–767.

AWWA, 1974. AWWA standard for granular activated carbon. J. Am. Water Works Assoc. 66 (11), 672–681.

Bichsel, Y., von Gunten, U., 1999. Oxidation of iodide and hypoiodous acid in the disinfection of natural waters. Environ. Sci. Technol. 33 (22), 4040–4045.

Bichsel, Y., von Gunten, U., 2000a. Hypoiodous acid: kinetics of the buffer-catalyzed disproportionation. Water Res. 34 (12), 3197–3203.

Bichsel, Y., von Gunten, U., 2000b. Formation of iodo-trihalomethanes during disinfection and oxidation of iodide-containing waters. Environ. Sci. Technol. 34 (13), 2784–2791.

Brown, J., Hammond, D., Wilkins, B.T., 2008. Handbook for Assessing the Impact of a Radiological Incident on Levels of Radioactivity in Drinking Water and Risks to Operatives at Water Treatment Works. Public Health England. http://www.hpa.org.uk/webc/HPAwebFile/HPAweb_C/1215762210590 (accessed 07.23.13.).

Criquet, J., Allard, S., Salhi, E., Joll, C.A., Heitz, A., von Gunten, U., 2012. Iodate and iodo-trihalomethane formation during chlorination of iodide-containing waters: role of bromide. Environ. Sci. Technol. 46 (13), 7350–7357.

Davis, J.A., Fox, P.M., Fuhrmann, M., 2009. Redox and Sorption Reactions of Iodine and Cesium during Transport through Aquifer Sediments (NUREG/CR-6977). Unites States Nuclear Regulatory Commission. http://www.nrc.gov/reading-rm/doc-collections/nuregs/contract/cr6977/ (accessed 04.12.14.).

Ding, G., Zhang, X., 2009. A picture of polar iodinated disinfection byproducts in drinking water by (UPLC/)ESI-tqMS. Environ. Sci. Technol. 43 (24), 9287–9293.

Gong, T., Zhang, X., 2013. Determination of iodide, iodate and organo-iodine in waters with a new total organic iodine measurement approach. Water Res. 47 (17), 6660–6669.

Hansen, V., Yi, P., Hou, X., Aldahan, A., Roos, P., Possnert, G., 2011. Iodide and iodate (129I and 127I) in surface water of the Baltic Sea, Kattegat and Skagerrak. Sci. Total Environ. 412–413 (0), 296–303.

Hua, G., Reckhow, D.A., Kim, J., 2006. Effect of bromide and iodide ions on the formation and speciation of disinfection byproducts during chlorination. Environ. Sci. Technol. 40 (9), 3050–3056.

Ikeda, N., Tanaka, K., 1975. Column chromatographic separation of radioactive tellurate, tellurite, iodide and iodate by active charcoal. J. Chromatogr. A 114 (2), 389–395.

Ikemoto, T., Magara, Y., 2011. Measures against impacts of nuclear disaster on drinking water supply systems in Japan. Water Pract. Technol. 6 http://dx.doi.org/10.2166/wpt.2011078.

Jones, D.B., Saglam, A., Triger, A., Song, H., Karanfil, T., 2011. I-THM formation and speciation: preformed monochloramine versus prechlorination followed by ammonia addition. Environ. Sci. Technol. 45 (24), 10429–10437.

Jones, D.B., Saglam, A., Song, H., Karanfil, T., 2012. The impact of bromide/iodide concentration and ratio on iodinated trihalomethane formation and speciation. Water Res. 46 (1), 11–20.

Kosaka, K., Asami, M., Kobashigawa, N., Ohkubo, K., Terada, H., Kishida, N., Akiba, M., 2012. Removal of radioactive iodine and cesium in water purification processes after an explosion at a nuclear power plant due to the Great East Japan Earthquake. Water Res. 46 (14), 4397–4404.

Kumar, K., Day, R.A., Margerum, D.W., 1986. Atom-transfer redox kinetics: general-acid-assisted oxidation of iodide by

chloramines and hypochlorite. Inorg. Chem. 25 (24), 4344–4350.
Lettinga, G., 1972. Radioactivity and Water Supplies. Delft, the Netherlands.
Matsui, Y., Ando, N., Yoshida, T., Kurotobi, R., Matsushita, T., Ohno, K., 2011. Modeling high adsorption capacity and kinetics of organic macromolecules on super-powdered activated carbon. Water Res. 45 (4), 1720–1728.
Plewa, M.J., Wagner, E.D., Richardson, S.D., Thruston, A.D., Woo, Y.-T., McKague, A.B., 2004. Chemical and biological characterization of newly discovered iodoacid drinking water disinfection byproducts. Environ. Sci. Technol. 38 (18), 4713–4722.
Richardson, S.D., Fasano, F., Ellington, J.J., Crumley, F.G., Buettner, K.M., Evans, J.J., Blount, B.C., Silva, L.K., Waite, T.J., Luther, G.W., McKague, A.B., Miltner, R.J., Wagner, E.D., Plewa, M.J., 2008. Occurrence and mammalian cell toxicity of iodinated disinfection byproducts in drinking water. Environ. Sci. Technol. 42 (22), 8330–8338.
Siddiqui, M., Zhai, W., Amy, G., Mysore, C., 1996. Bromate ion removal by activated carbon. Water Res. 30 (7), 1651–1660.
Summers, R.S., Fuchs, F., Sontheimer, H., 1989. The fate and removal of radioactive iodine in the aquatic environment. In: MacCarthy, I.H.S.a.P. (Ed.), Aquatic Humic Substances: Influence on Fate and Treatment of Pollutants, Advances in Chemistry Series, Number 219. American Chemical Society, Washington DC.
Tate, C.H., Chow, B.M., Clark, R.R., Grams, N.E., Hashimoto, L.K., 1986. EPA Method Study 32: Method 450.1-Total Organic Halide (TOX). Environmental Monitoring and System Laboratory, USEPA, Cincinnati, Ohio, USA. http://www.epa.gov/nscep/index.html (accessed 05.18.14.).

Repeated Dose and Reproductive/Developmental Toxicity of Perfluorododecanoic Acid in Rats

Hina Kato,[1] Sakiko Fujii,[2] Mika Takahashi,[1] Mariko Matsumoto,[1] Mutsuko Hirata-Koizumi,[1] Atsushi Ono,[1] Akihiko Hirose[1]

[1]Division of Risk Assessment, Biological Safety Research Center, National Institute of Health Sciences, 1-18-1 Kamiyoga, Setagaya-Ku, Tokyo 158–8501, Japan

[2]Safety Research Institute for Chemical Compounds Co., Ltd., 363-24 Sin-ei, Kiyota-ku, Sapporo, Hokkaido 004–0839, Japan

Received 19 November 2013; revised 25 March 2014; accepted 4 April 2014

ABSTRACT: Perfluoroalkyl carboxylic acids (PFCAs) are a series of environmental contaminants that have received attention because of their possible adverse effects on wildlife and human health. Although many toxicological studies have been performed on perfluorooctanoic acid with carbon chain length C8, available toxicity data on PFCAs with longer chains are still insufficient to evaluate their hazard. A combined repeated dose and reproductive/developmental toxicity screening study for perfluorododecanoic acid (PFDoA; C12) was conducted in accordance with OECD guideline 422 to fill these toxicity data gaps. PFDoA was administered by gavage to male and female rats at 0.1, 0.5, or 2.5 mg/kg/day. The administration of PFDoA at 0.5 and 2.5 mg/kg/day for 42–47 days mainly affected the liver, in which hypertrophy, necrosis, and inflammatory cholestasis were noted. Body weight gain was markedly inhibited in the 2.5 mg/kg/day group, and a decrease in hematopoiesis in the bone marrow and atrophic changes in the spleen, thymus, and adrenal gland were also observed. Regarding reproductive/developmental toxicity, various histopathological changes, including decreased spermatid and spermatozoa counts, were observed in the male reproductive organs, while continuous diestrous was observed in the females of the 2.5 mg/kg/day group. Seven of twelve females receiving 2.5 mg/kg/day died during late pregnancy while four other females in this group did not deliver live pups. No reproductive or developmental parameters changed at 0.1 or 0.5 mg/kg/day. Based on these results, the NOAELs of PFDoA were concluded to be 0.1 mg/kg/day for repeated dose toxicity and 0.5 mg/kg/day for reproductive/developmental toxicity.

Keywords: perfluorododecanoic acid; repeated dose toxicity; reproductive toxicity; developmental toxicity; screening test; rat; perfluoroalkyl carboxylic acid

INTRODUCTION

Perfluoroalkyl carboxylic acids (PFCAs) are a series of environmental contaminants that have recently received attention because of their possible effects on wild life and human health. They have been widely used as processing aids in the manufacture of fluoropolymers and as additives and components in consumer and industrial products (Prevedouros et al., 2006). Major sources of environmental pollution are considered to be fluoropolymer manufactures (Prevedouros et al., 2006). The stability and nonbiodegradability of PFCAs

Correspondence to: A. Hirose; e-mail: hirose@nihs.go.jp

Contract grant sponsor: Health and Labour Sciences Research Grant, Ministry of Health, Labour and Welfare, Japan.

Contract grant numbers: H22-Kenki-Ippan-006, H25-Kenki-Ippan-007

Contract grant sponsor: Ministry of Health, Labour and Welfare, Japan

Published online 00 Month 2014 in Wiley Online Library (wileyonlinelibrary.com). DOI: 10.1002/tox.21996

allow them to be persistent in the environment (Lau et al., 2007).

Many toxicological studies have been performed on the 8-carbon chain length PFCA, perfluorooctanoic acid (PFOA), which was the most widely used PFCA at least until the PFOA Stewardship Program was launched by the United States Environmental Protection Agency and eight major industrial companies in 2006 (US EPA, 2013). Repeat-dose toxicity studies of PFOA in rodents revealed a steep dose-response curve for mortality, reduced body weight, and hepatocellular hypertrophy and necrosis (Griffith et al., 1980; Perkins et al., 2004; UK COT, 2006). The incidences of hepatocellular adenomas, Leydig cell tumors, and pancreatic acinar cell tumors were shown to be increased in a 2-year bioassay of PFOA in rats (Biegel et al., 2001). The developmental and hormonal effects and immunotoxic potential of PFOA have also been established in rodents (Lau et al., 2007). The lowest NOAEL of PFOA was 0.06 mg/kg/day based on its effects on the liver in a 13-week feeding study in rats (Perkins et al., 2004).

Recent studies have been extended to other PFCAs, which can be used as alternatives to PFOA. Findings have indicated that the toxic potency of PFCAs increases with lengthening of the carbon chain, at least up to C9 (Permadi et al., 1993; Kudo et al., 2006). Since the bioaccumulation potential of PFCAs has also been reported to increase depending on their carbon number (Martin et al., 2003), long-chain PFCAs may cause serious environmental and/or human health concerns in the future; however, available toxicity data on such long-chain PFCAs are still insufficient to evaluate the hazard.

To evaluate longer chain PFCAs, the Ministry of Health, Labour and Welfare, Japan, conducted combined repeat dose and reproductive/developmental toxicity screening tests on several long-chain PFCAs (carbon chain lengths C11 to C18) under the Japanese safety programmes for existing chemicals between 2007 and 2011. We previously reported the results for perfluorooctadecanoic acid [PFOdA (C18)], which demonstrated that the toxic potency of PFOdA was relatively low, compared to the other PFCAs; the NOAELs were 40 mg/kg/day for repeated dose toxicity and 200 mg/kg/day for reproductive/developmental toxicity (Hirata-Koizumi et al., 2012). This study reported the recently obtained results for perfluorododecanoic acid [PFDoA (C12); CAS No. 16517-11-6].

PFDoA is a white powder with a melting point of 107–109°C. It has been reported that PFDoA was detected in the influent, effluent, or sludge in sewage and also in industrial wastewater treatment plants in Japan, Thailand, and Australia (Clara et al., 2008; Murakami et al., 2009; Kunacheva et al., 2011), in the water, sediment, or soil of rivers in Japan, China, and Australia (Nishikoori et al., 2011; Thompson et al., 2011; Wang et al., 2012), and in house dust and indoor air in Norway (Haug et al., 2011). PFDoA has been detected in various wildlife including the albatross, harbor seals, and porpoises in many different geographic locations throughout the world (Hoff et al., 2004; Tao et al., 2006; Van de Vijver et al., 2007; Ahrens et al., 2009; Thompson et al., 2011). PFDoA was found at the levels of a few pg/mL to hundreds of pg/mL in the blood of humans in various parts of the world (Guruge et al., 2005; Falandysz et al., 2006; Harada et al., 2011; Haug et al., 2009; Olsen et al., 2012) and at <10–41 pg/mL in breast milk in East Asia (Fujii et al., 2012).

The concentration of PFDoA in the river sediment or soil and in wildlife exceeded that of PFOA, which may reflect the lower water solubility and higher bioaccumulative properties of PFDoA (Martin et al., 2003; Inoue et al., 2012). Although there is no data available on the production volume and application, PFDoA sources may not only be from the manufacture and use of PFDoA, but also from where PFDoA is present as an impurity or where substances may degrade to form PFDoA (Prevedouros et al., 2006).

PFDoA was recently reported to affect the liver, leading to lipidosis and widespread disintegrated cell systems, and inhibited steroidogenesis in the testis and ovary in rats (Shi et al., 2007, 2009a,b, 2010a,b; Zhang et al., 2008; Ding et al., 2009); however, no data are available on how PFDoA affects other organs, reproductive performance, and development. The results of the combined repeated dose and reproductive/developmental toxicity screening test described here may provide a more comprehensive toxicity profile of PFDoA than has been reported previously.

MATERIALS AND METHODS

This study was conducted in accordance with OECD guideline 422 "Combined Repeated Dose Toxicity Study with the Reproduction/Developmental Toxicity Screening Test" (OECD, 1996) at the Safety Research Institute for Chemical Compounds (Sapporo, Japan). All procedures involving the use and care of animals complied with the principles for Good Laboratory Practice (MOE et al., 2008) and applicable animal welfare regulations ["Act on Welfare and Management of Animals" (Japanese Animal Welfare Law, 2006), "Standards Relating to the Care, Management of Laboratory Animals and Relief of Pain" (MOE, 2006), and "Guidelines for Animal Experimentation" (JALAS, 1987)].

Animals and Housing Conditions

Crl:CD(SD) rats (8-week-old) were purchased from Atsugi Breeding Center, Charles River Laboratories Japan, Inc. (Yokohama, Japan). They were maintained in an air-conditioned room with controlled temperature (22 ± 3°C) and humidity (50 ± 20%). Light was provided on a 12-h light/dark cycle (light: 8:00–20:00). Animals were housed in groups of two during the quarantine and acclimation periods, and after being assigned to each dose group, were reared individually, except for mating and nursing periods, in metal

bracket-type cages with wire-mesh floors.. Regarding pregnant animals, individual dams and litters were reared from day 17 of gestation to day 4 of nursing using wood chips as bedding (White Flake; Charles River Laboratories Japan). All animals were fed *ad libitum* with a standard rat diet (CRF-1; Oriental Yeast, Tokyo, Japan), and had free access to tap water (Sapporo, Japan).

Rats were acclimated to the laboratory for 14 days, during which general conditions were observed once a day and body weights were measured on the day of receipt, the 8th day of acclimation, and the end of acclimation. No abnormality was seen in the general state or weight in either animal. Vaginal smears were prepared daily for female animals in order to examine the estrous cycle for 9 days before animals were assigned to each group. Abnormalities were identified in two females. Animals found to be in good health and showing normal estrous cycles were divided into each dose group by stratified random sampling to equalize the mean body weight. The body weights of animals selected for the study were from 368 to 424 g in males and from 228 to 279 g in females.

Chemicals and Dosing

PFDoA was purchased from Exfluor Research Corporation (TX, USA). The PFDoA (Lot No. 4103) used in this study was 97 % pure, and was kept in an airtight container in a cold and dark place (2–9°C). The test article was suspended in a 0.5% aqueous solution of carboxymethylcellulose sodium (CMC-Na; Maruishi Pharmaceutical, Osaka, Japan), and administered to the animals by gastric intubation with a disposable gastric tube and disposable syringe. Before the start of the study, the stability of PFDoA in a 0.5% CMC-Na aqueous solution at concentrations of 0.01 and 100 mg/mL was confirmed after 4-h storage at room temperature following a 15-day refrigerated storage; therefore, dosing solutions were prepared at least once every 15 days throughout the study and were kept in a cool (2.0–7.2°C) and dark place under airtight conditions until dosing. The concentrations of PFDoA in the formulations were analyzed at the first and last preparation using high-performance liquid chromatography-tandem mass spectrometry, and were confirmed to be 96.4–99.0% of the target.

Experimental Design

Rats were administered PFDoA daily by repeated oral administration. The dose levels were determined based on the results of a 14-day dose-finding study, in which the liver weight was increased at all doses (1 mg/kg/day and above), and more clear toxic effects, including inhibition of body weight gain, changes in blood biochemical, and hematological parameters and brown discoloration of the liver, were observed in rats given 3 and 5 mg PFDoA/kg/day. Considering the longer administration period in the present combined study, the maximum dose of PFDoA was set at 2.5 mg/kg/day, and 0.1 and 0.5 mg/kg/day were derived by one-fifth divisions. The daily application volume (10 mL/kg body weight) was calculated according to the latest body weight. Control rats were given the same volume of vehicle alone.

Twelve males in each dose group (0, 0.1, 0.5, and 2.5 mg/kg/day) were dosed for a total of 42 days, beginning 14 days before mating. Seven males in the control and 2.5 mg/kg/day groups and all males in the 0.1 and 0.5 mg/kg/day groups were necropsied the day after day 42 of the dose (main group). The remaining five males in the control and 2.5 mg/kg/day groups were assigned to a recovery group, and after 42-day administration, they were kept without administration for 14 days (recovery period) and then necropsied. Twelve females/dose were dosed from 14 days prior to mating (main group). The pregnant females were dosed for gestation and nursing periods until 5 days after delivery and then necropsied on day 6 of nursing. Pregnant females which did not deliver by day 25 of gestation and females which showed abnormal delivery (stillbirth) were necropsied on day 26 of gestation and on day 0 of nursing, respectively. As a recovery group, other five females per dose were dosed with 0 or 2.5 mg PFDoA/kg/day for a total of 42 days without mating, and then kept without administration for 14 days (recovery period). All females in the recovery group were necropsied on the day after the 14-day recovery period, and therefore, females given PFDoA without mating were not examined fully at the end of administration period.

The first date of administration was defined as day 1 of the doing. In the main group females, the day of successful copulation was designated as day 0 of gestation and the end of deliver as day 0 of nursing or postnatal day (PND) 0. In recovery group males and females, the day following 42-day administration was defined as day 1 of recovery period.

Observation and Examination

Repeated Dose Toxicity Data

In all animals, general status, including life or death, appearance and behavior, of individual rats was observed twice daily during administration period (before and after the administration) and during the recovery period (morning and afternoon), and once in the morning of the day of necropsy. In addition, detailed clinical observations were conducted using a standardized scoring system for all of the animals before start of administration and once a week throughout the administration and recovery periods. Food consumption and body weight were measured at regular intervals throughout the administration and recovery periods.

Functional observations were performed on day 40 of the administration and on day 8 of recovery periods for males and for females of the recovery group, and on day 4 of nursing for females of main group. Subjects for the observations were 5 males/dose selected to approximate to the mean body weight of each dose group, 5 females/dose in recovery group

and 5 females/dose having delivered earlier in the main group. Evaluations were conducted using a predetermined standardized scoring system, as follows: (i) Sensorimotor reactivity to visual, tactile, auditory, pain, proprioceptive stimuli, and air righting reflex was assessed on an examination table, (ii) Forelimb and hindlimb grip strength was measured three times with a CPU gauge (Aikoh Engineering, Osaka, Japan), and (iii) Spontaneous motor activity was recorded for 1 h at intervals of 10 min using an automated activity monitor system [SUPERMEX and CompAct AMS (Muromachi Kikai, Tokyo, Japan)].

Urine was collected at the end of the administration and recovery periods in a nonfasted condition from five males per dose selected for functional observations and from five females per dose in the recovery group in the metabolism cage (KN-646, B-1 type, Natsume Seisakusho, Tokyo, Japan). Fresh urine (3 h) was examined for pH, protein, glucose, ketone body, urobilinogen, bilirubin, occult blood, and color, and urine volume and specific gravity were measured using collected urine (21 h).

Blood samples were collected for hematology and blood biochemistry from the abdominal aorta at necropsy under ether anesthesia after starvation for 16–22 h. In the main group, five males per dose not used in the functional observations and five females per dose used in the functional observations were selected for blood sampling. All animals in the recovery group were subjected to the blood sampling. One portion of the blood was treated with ethylenediaminetetraacetic acid dipotassium (EDTA-2K,TERUMO CORPORATION., Tokyo, Japan) and examined for the red blood cell count (RBC), hematocrit (HCT), hemoglobin (HGB), mean corpuscular volume (MCV), mean corpuscular hemoglobin (MCH), mean corpuscular hemoglobin concentration (MCHC), reticulocyte, platelet count, white blood cell count (WBC), and differential count of white blood cells. Prothrombin time (PT), and activated partial thromboplastin time (APTT) were measured using plasma separated from another blood sample treated with 3.8% sodium citrate. Plasma obtained from blood treated with heparin sodium [HEPARIN SODIUM INJECTION-N "Ajinomoto", 1000 unit/mL (AJINOMOTO CO., INC., Tokyo, Japan)] was analyzed for aspartate aminotransferase (AST) and glucose. Serum prepared by centrifuging the blood collected in tubes filled with a serum separation agent (SEPACLEAN-A, EIKEN CHEMICAL CO., LTD., Tokyo, Japan) was analyzed for alanine aminotransferase (ALT), alkaline phosphatase (ALP), γ-glutamyltranspeptidase (γ-GTP), total cholesterol (T-Cho), triglycerides (TG), total bilirubin (T-Bil), blood urea nitrogen (BUN), creatinine (Crea), sodium (Na), potassium (K), chlorine (Cl), calcium (Ca), inorganic phosphorus (IP), total protein (TP), protein fraction ratio, albumin/globulin (A/G) ratio, and albumin.

All surviving animals were euthanized by exsanguination after blood was collected under deep ether anesthesia and the external surfaces and organs and tissues of the whole body were examined macroscopically. The brain, pituitary gland, thyroid, heart, liver, kidney, spleen, adrenal gland, thymus, testes, epididymides, and ovaries were then weighed. The following organs and tissues were fixed and stored in 10% neutral-buffered formalin: the brain (cerebrum, cerebellum, and pons), spinal cord, pituitary gland, thymus, thyroid (including parathyroid), adrenal gland, spleen, heart, esophagus, stomach, liver, pancreas, duodenum, jejunum, ileum (including Peyer's patch), cecum, colon, rectum, trachea, lung, kidney, urinary bladder, prostate, seminal vesicle (including the coagulating gland), ovary, uterus (horn part and jugular), mammary gland (right abdomen), femur (right, including bone marrow), mesenteric lymph nodes, submandibular lymph nodes, sciatic nerve, and grossly abnormal tissues (including the boundary with normal tissues). The eyeball and Harderian gland were fixed and preserved with Davidson's fixative solution. The testis and epididymis were fixed with Bouin's solution and preserved in 70% ethanol. The lungs were fixed with immersion following the injection of fixing solution. In principle, organs with right and left parts were both fixed and preserved.

Histopathological examinations were conducted on the preserved organs and tissues of five males and five females in the control and high dose groups, and also dead and euthanized animals during the study. All grossly abnormal tissues were also histopathologically examined regardless of the dose groups. Since treatment-related gross or histopathological abnormalities in the high dose group were observed in the forestomach, glandular stomach, pancreas, liver, testis, epididymis, prostate gland, seminal vesicle, coagulating gland, uterine horn part, spleen, thymus, born marrow, and adrenal gland, these organs from all animals in all groups were examined histopathologically. The organs were sectioned after paraffin embedding, stained with hematoxylin–eosin, and examined under a light microscope. To confirm the findings of the liver, specimens stained with Hall stain and Oil red O were additionally prepared and examined microscopically.

Reproductive/Developmental Toxicity Data

The estrous cycle of all females was evaluated by sampling the vaginal lavage daily from the first day of administration until evidence of copulation in the main group and until the necropsy day in the recovery group. Vaginal smear specimens made by the Giemsa stain were observed under an optical microscope. Females having repeated 4–6 day estrous cycles were judged to have normal estrous cycles.

Each female in the main group was transferred to the home cage of a randomly chosen male from the same exposure group on day 14 of administration, and cohabited on a 1 : 1 basis until successful copulation occurred or a mating period of 2 weeks had elapsed. The presence of sperm in the vaginal smear and/or a vaginal plug was considered as evidence of successful mating. Gestation was confirmed by the

presence of delivery and by counting the number of implantation sites in the uterus at necropsy. Following confirmation of mating, females were returned to their home cages and allowed to deliver spontaneously and nurse their pups. They were checked at least three times daily (9:00, 13:00, and 17:00) on days 21–25 of gestation, and the day on which dams held their pups under the abdomen in the nest by 9:00 was designated as the end of delivery. Gestational length was recorded, and the copulation index, fertility index, and gestation index were computed for each dose group.

All live and dead pups born were counted on PND 0, and the live birth index was calculated for each litter. Live pups were sexed and examined grossly on PNDs 0 and 4. Sex ratios were calculated for each litter. They were observed daily for general appearance and behavior, and the body weight of live pups was recorded on PNDs 0, 1, and 4. The viability index on PND 4 was calculated for each litter. All pups were euthanized on PND 4 by the inhalation of carbon dioxide and subjected to a gross external and internal (include the oral cavity) observation.

At necropsy of maternal animals, the numbers of corpora lutea and implantation in the uterus were recorded, and the implantation index and delivery index were calculated for each litter.

Statistical Analysis

The trend for detailed clinical and functional observations of each group, qualitative parameters of urinalysis, specific gravity of urine, and histopathological findings with multiple grades was evaluated by the Kruskal-Wallis test. If significant differences were identified ($p \leq 0.10$), data were compared between the control and each dosage group using the Mann-Whitney U test. The incidence of females with normal estrous cycles, copulation, fertility, and gestation indices, and histopathological findings with a single grade were analyzed using the chi-square test. If significant differences were found ($p \leq 0.10$), the data were compared between the control and each dosage group using the chi-square two sample test or the Fisher's exact probability test.

The mean and standard deviation were calculated for the other parameters and evaluated by the Bartlett's test for homogeneity of variances. The live birth index, neonatal sex ratio, viability index, and body weight of male and female pups were similarly analyzed using the litter as the experimental unit. When homogeneity was recognized ($p > 0.05$), a one-way analysis of variance was applied and data without homogeneity ($p \leq 0.05$) were subjected to the Kruskal-Wallis test. If a significant difference was identified ($p \leq 0.10$), the Dunnett's test or the Mann-Whitney test was used for pairwise comparisons between the control and individual treatment groups.

All statistical analyses comparing the control and individual treatment groups were conducted using the 5% level of probability as the criterion for significance.

RESULTS

Clinical and Functional Observations

In the 2.5 mg/kg/day group, soft feces was observed in one male on days 35–42 of the administration period and in another male only on day 4 of the recovery period. Although no deaths were observed in males, four females given 2.5 mg PFDoA/kg/day were found dead on days 18–22 of gestation. Hypothermia and vaginal hemorrhage were observed before death in one female. Three females were euthanized in the 2.5 mg/kg/day group due to a moribund condition on days 18–20 of gestation. In addition, two females were euthanized on day 26 of gestation because they did not deliver any pups, and two females were euthanized on nursing day 0 because of abnormal delivery (all pups stillborn). No clinical signs of toxicity were observed in females in the recovery group.

In detailed clinical observations, no significant difference was observed between the control and PFDoA-treated groups at any observation point. Although no significant differences were observed in functional observations for males on day 42 of the administration period between the control and PFDoA-treated groups, a significant decrease in forelimb grip strength was noted in males in the 2.5 mg/kg/day group at the end of the recovery period (Table I). A similar change was also observed in females of the recovery group. In females in the main group, the results of the 2.5 mg/kg/day group were exempt from statistical evaluation because only one female normally delivered pups and survived to the day of the functional observations (day 4 of nursing). Forelimb grip strength was slightly higher in this female than in control females. No significant change was observed in hindlimb grip strength in any of the treatment groups in either sex. In females given 2.5 mg PFDoA/kg/day in the recovery group, a significant decrease in motor activity was observed at 0–10 min, 10–20 min, and 20–30 min on week 6 of administration. Total motor activity for 60 min was also significantly decreased (Table I). Such an effect was not found on week 2 of the recovery period. No significant changes were observed in motor activity in any other groups.

Body Weight

Body weight was significantly lower in males at 2.5 mg/kg/day than in the controls from day 21 to the end of the 42-day administration period, and it remained significantly lower until the end of the 14-day recovery period (Fig. 1). Body weight in females in the recovery group showed similar time-dependent changes to those observed in the males, as shown in Figure 1. Body weight in females in the main group was significantly decreased at 2.5 mg/kg/day through the gestation period (Fig. 2). One female that normally delivered pups in the 2.5 mg/kg/day group had a lower body weight than the controls during the nursing period.

TABLE I. Grip strength and motor activity in male and female rats administered PFDoA

Dose (mg/kg/day)			0 (control)	0.1	0.5	2.5
MALES						
Number of animals examined			5	5	5	5
Administration week 6						
	Grip strength (g)	Forelimb	1459.28 ± 99.35	1532.14 ± 197.47	1632.80 ± 372.40	1313.72 ± 312.91
		Hindlimb	673.92 ± 240.73	636.16 ± 155.70	671.26 ± 84.61	526.92 ± 100.23
	Total motor activity	(60 min)	1459.3 ± 99.4	1169.4 ± 487.4	1340.0 ± 831.2	732.8 ± 442.6
Recovery week 2						
	Grip strength (g)	Forelimb	1576.54 ± 290.26			1217.00 ± 147.46*
		Hindlimb	669.16 ± 85.59			531.26 ± 119.71
	Total motor activity	(60 min)	1171.2 ± 344.9			9961.4 ± 362.2
FEMALES						
Number of animals examined			5	5	5	1
Day 4 of nursing (Main group)						
	Grip strength (g)	Forelimb	943.68 ± 140.49	922.20 ± 137.48	904.68 ± 124.73	1236.70[a]
		Hindlimb	502.66 ± 80.17	475.08 ± 88.55	478.46 ± 41.24	413.00[a]
	Total motor activity	(60 min)	1216.2 ± 234.2	1222.6 ± 494.5	1240.2 ± 853.1	1145.0[a]
Number of animals examined			5			5
Administration week 6 (Recovery group)						
	Grip strength (g)	Forelimb	1236.20 ± 260.53			998.20 ± 137.67
		Hindlimb	582.20 ± 51.34			472.54 ± 112.04
	Total motor activity	(60 min)	2785.6 ± 1000.2			1044.2 ± 563.3**
Recovery week 2 (Recovery group)						
	Grip strength (g)	Forelimb	1233.28 ± 221.67			834.58 ± 87.45**
		Hindlimb	630.68 ± 70.19			537.22 ± 105.37
	Total motor activity	(60 min)	1933.0 ± 1171.4			1117.8 ± 764.9

*Significantly different from the control, at $p \leqq 0.05$.
**Significantly different from the control, at $p \leqq 0.01$.
[a]Data from only one animal. In this group, other females did not deliver pups normally or survive to the day of the functional observations.

Food Consumption

A remarkable and significant decrease in food consumption was observed on days 28, 35, and 42 of the administration period at 2.5 mg/kg/day in males. However, no significant decreases were noted in food consumption in the 0.1 and 0.5 mg/kg/day groups. During the recovery period, no significant difference was observed in food consumption between the control and PFDoA-treated groups in males.

Females given 2.5 mg PFDoA/kg/day in the main group also consumed a significantly smaller amount of food from day 3 through day 20 of gestation. The amount of food consumed by one female that normally delivered pups in this group was lower than that of the control group during the nursing period. Food consumption in females in the 2.5 mg/kg/day recovery group showed similar time-dependent changes to those in the males.

Urinalysis

No significant difference was seen in any urinalysis parameters between the control and PFDoA-treated groups either at the end of the administration period or at the end of the recovery period.

Hematology

MCV and the reticulocyte ratio were significantly lower and MCHC was significantly higher in males given 2.5 mg

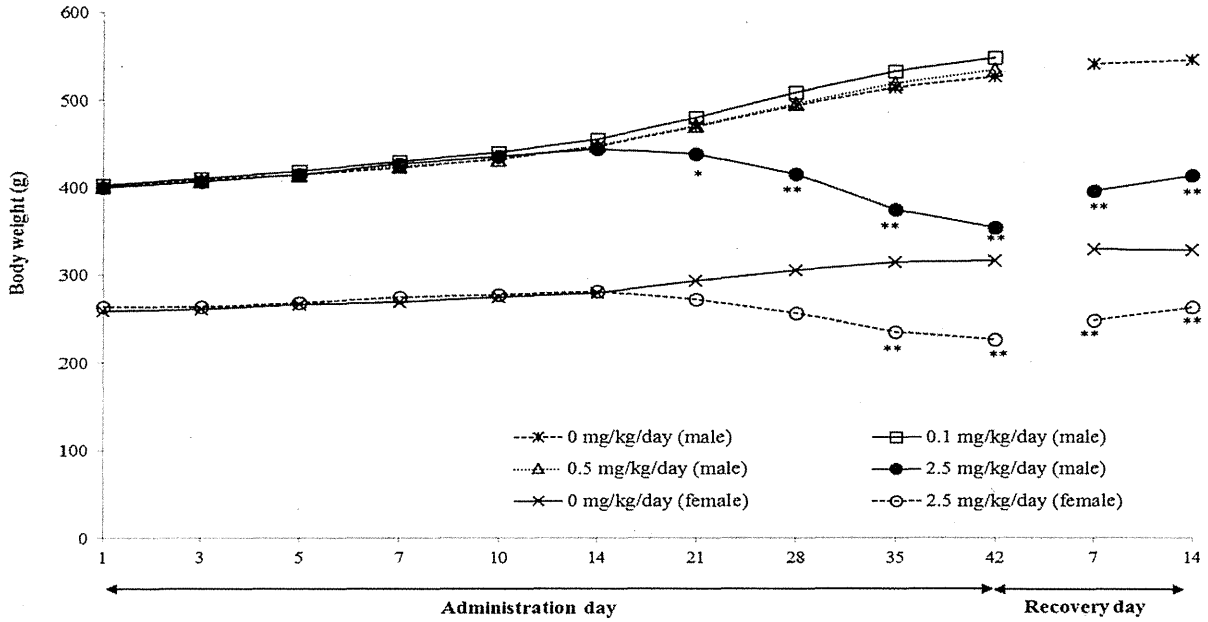

Fig. 1. Body weight changes in male rats in the main and recovery groups and female rats in the recovery group in the combined repeated dose toxicity study with the reproduction/developmental toxicity screening test for perfluorododecanoic acid. *Significantly different from the 0 mg/kg/day group at $p \leq 0.05$, **Significantly different from the 0 mg/kg/day group at $p \leq 0.01$.

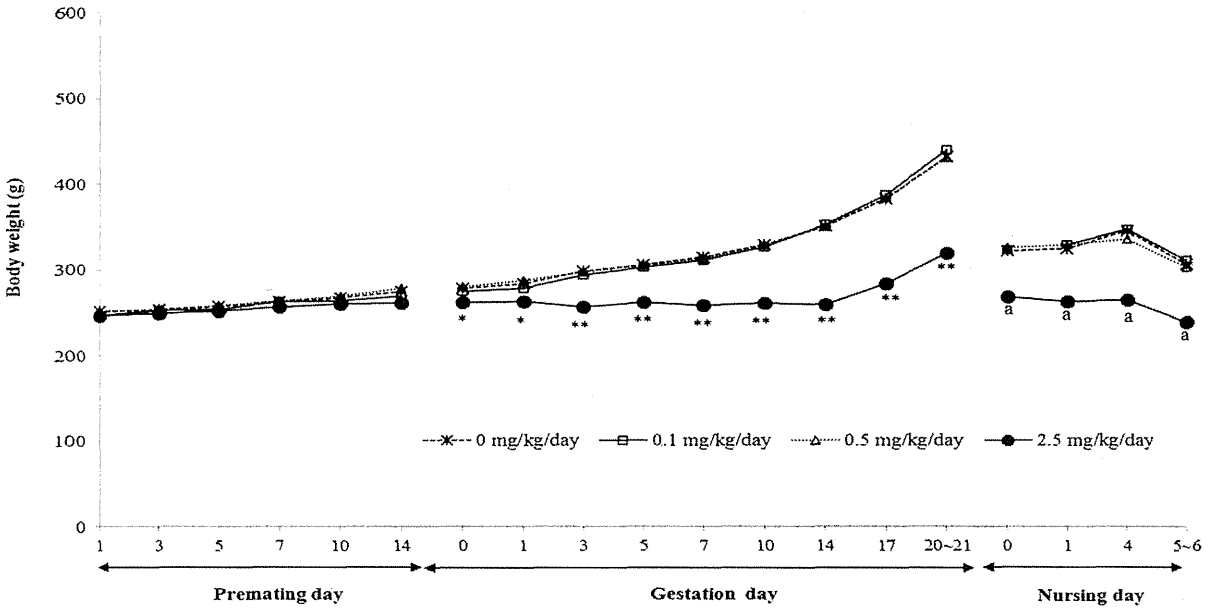

Fig. 2. Body weight changes in female rats in the main group in the combined repeated dose toxicity study with the reproduction/developmental toxicity screening test for perfluorododecanoic acid. *Significantly different from the 0 mg/kg/day group at $p \leq 0.05$, **Significantly different from the 0 mg/kg/day group at $p \leq 0.01$. a: The data were exempt from statistical evaluation because only one female normally delivered pups.

PFDoA/kg/day than in the control group at the end of the administration period (Table II). In this dose group, significant decreases were noted in WBC, RBC, HGB, HCT, and lymphocyte, monocyte, and eosinophil counts on a differential counts of WBC, and a significant increase was observed in the reticulocyte counts at the end of the recovery period.

Many changes, including decreases in HCT, MCV, and the reticulocyte count and an increase in MCHC, were found in one female given 2.5 mg/kg/day, as shown in Table II. In the 0.1 and 0.5 mg/kg/day groups, no significant changes were found in any parameters. In the recovery group, HGB, HCT, MCV, and MCH were significantly lower, while the neutrophil differential count of WBC was significantly higher in females given 2.5 mg PFDoA/kg/day than in the control group.

Blood Biochemistry

Serum TP and albumin levels were significantly decreased in males at 2.5 mg/kg/day at the completion of the administration period (Table III). Significant increases were observed in the albumin and γ-globulin ratios in the protein fraction, as well as a significant decrease in the α_1-globulin ratio at 2.5 mg/kg/day and a significant decrease in the α_2-globulin ratio at 0.5 mg/kg/day and above. ALP activity was

TABLE II. Hematological findings in male and female rats administered PFDoA

	Main Group				Recovery Group	
Dose (mg/kg/day)	0 (control)	0.1	0.5	2.5	0 (control)	2.5
MALES						
Number of animals examined	5	5	5	5	5	5
Red blood cells (10^4/μL)	918 ± 37	914 ± 18	927 ± 31	943 ± 58	978 ± 56	859 ± 41**
Hemoglobin (g/dL)	16.3 ± 0.6	16.2 ± 0.4	17.0 ± 0.6	16.1 ± 0.9	16.4 ± 0.6	14.2 ± 0.6**
Hematocrit (%)	46.3 ± 1.4	46.2 ± 1.6	48.2 ± 2.2	44.0 ± 1.9	46.0 ± 1.3	40.3 ± 13.0**
MCV (fL)	50.5 ± 2.8	50.6 ± 2.2	52.0 ± 2.0	46.7 ± 1.6	47.1 ± 1.6	47.0 ± 1.4
MCH (pg)	17.8 ± 1.1	17.7 ± 0.7	18.3 ± 0.5	17.1 ± 0.4	16.8 ± 0.4	16.5 ± 0.4
MCHC (g/dL)	35.2 ± 0.3	35.0 ± 0.4	35.2 ± 0.5	36.7 ± 0.8**	35.7 ± 0.5	35.2 ± 0.5
Reticulocytes (%)	3.18 ± 0.47	3.26 ± 0.55	3.35 ± 0.63	1.17 ± 0.67**	3.15 ± 0.31	4.63 ± 0.56**
Platelets (10^4/μL)	124.8 ± 8.6	112.5 ± 11.8	118.0 ± 9.0	116.7 ± 33.2	127.6 ± 15.6	169.9 ± 41.2
White blood cells (10^2/μL)	113.4 ± 28.2	148.2 ± 33.9	108.4 ± 19.6	135.0 ± 36.9	139.8 ± 14.2	112.5 ± 6.9**
Neutrophils (10^2/μL)	16.8 ± 4.1	17.9 ± 6.2	13.8 ± 3.1	21.2 ± 8.6	19.3 ± 8.4	15.3 ± 5.0
Lymphocytes (10^2/μL)	90.6 ± 24.5	123.7 ± 30.6	89.8 ± 17.9	108.0 ± 32.4	112.5 ± 15.0	93.0 ± 6.0*
Monocytes (10^2/μL)	4.24 ± 1.22	4.28 ± 0.65	3.56 ± 1.18	4.76 ± 3.85	5.36 ± 1.90	2.54 ± 0.78*
Eosinophils (10^2/μL)	1.68 ± 0.78	2.26 ± 0.73	1.22 ± 0.55	1.00 ± 0.58	2.60 ± 0.62	1.56 ± 0.56*
Basophils (10^2/μL)	0.04 ± 0.09	0.04 ± 0.05	0.02 ± 0.04	0.06 ± 0.09	0.06 ± 0.05	0.00 ± 0.00
PT (sec)	21.3 ± 4.3	22.7 ± 3.9	20.7 ± 3.5	19.1 ± 0.9	20.1 ± 3.4	18.5 ± 1.0
APTT (sec)	26.0 ± 2.3	26.9 ± 2.2	25.9 ± 1.6	22.0 ± 3.5	25.5 ± 4.5	23.0 ± 1.2
FEMALES						
Number of animals examined	5	5	5	1	5	5
Red blood cells (10^4/μL)	812 ± 24	828 ± 44	837 ± 26	803[a]	868 ± 27	836 ± 43
Hemoglobin (g/dL)	15.3 ± 0.5	15.5 ± 0.5	15.6 ± 0.4	14.5[a]	15.8 ± 0.4	14.2 ± 0.7**
Hematocrit (%)	44.6 ± 1.9	45.6 ± 1.5	45.2 ± 1.2	40.5[a]	45.2 ± 1.1	41.1 ± 2.2**
MCV (fL)	54.9 ± 2.2	55.1 ± 1.6	54.1 ± 1.7	50.4[a]	52.1 ± 1.6	49.2 ± 2.1*
MCH (pg)	18.8 ± 0.5	18.8 ± 0.6	18.6 ± 0.3	18.1[a]	18.3 ± 0.5	17.0 ± 0.6**
MCHC (g/dL)	34.3 ± 0.5	34.0 ± 0.3	34.4 ± 0.6	35.8[a]	35.1 ± 0.5	34.6 ± 0.4
Reticulocytes (%)	9.79 ± 1.26	10.20 ± 1.14	8.67 ± 1.46	4.05[a]	3.00 ± 0.56	4.00 ± 0.90
Platelets (10^4/μL)	124.3 ± 11.6	144.5 ± 9.9*	136.7 ± 9.5	143.0[a]	112.8 ± 14.3	118.8 ± 35.4
White blood cells (10^2/μL)	116.5 ± 34.4	101.9 ± 37.0	102.0 ± 17.4	95.7[a]	82.7 ± 24.7	104.9 ± 31.8
Neutrophils (10^2/μL)	41.0 ± 28.6	24.6 ± 13.8	28.6 ± 7.8	14.2[a]	10.1 ± 4.0	17.5 ± 5.2*
Lymphocytes (10^2/μL)	67.8 ± 14.9	70.2 ± 21.5	64.6 ± 9.0	72.3[a]	68.5 ± 20.7	81.1 ± 32.2
Monocytes (10^2/μL)	5.60 ± 1.39	5.50 ± 2.09	6.86 ± 2.58	8.20[a]	2.82 ± 0.84	5.18 ± 2.28
Eosinophils (10^2/μL)	2.02 ± 0.66	1.54 ± 0.76	1.90 ± 0.32	0.90[a]	1.28 ± 0.38	1.16 ± 0.73
Basophils (10^2/μL)	0.04 ± 0.05	0.06 ± 0.05	0.04 ± 0.05	0.10[a]	0.00 ± 0.00	0.02 ± 0.04
PT (sec)	18.7 ± 1.0	18.0 ± 0.8	17.8 ± 1.1	17.2[a]	17.4 ± 0.9	18.9 ± 4.6
APTT (sec)	20.4 ± 1.0	20.2 ± 1.2	20.7 ± 1.9	21.8[a]	18.9 ± 1.6	25.3 ± 8.6

Values are given as the mean ± S.D.

*Significantly different from the control, $p \leq 0.05$.

**Significantly different from the control, $p \leq 0.01$.

[a]Data from only one animal. In this group, other females did not deliver pups normally or survive to the end of the study.

TABLE III. Blood biochemical findings in male and female rats administered PFDoA

	Main Group				Recovery Group	
Dose (mg/kg/day)	0 (control)	0.1	0.5	2.5	0 (control)	2.5
MALES						
Number of animals examined	5	5	5	5	5	5
Total protein (g/dL)	5.62 ± 0.13	5.54 ± 0.24	5.50 ± 0.16	4.30 ± 0.43**	5.74 ± 0.11	4.70 ± 0.14**
Albumin (g/dL)	2.82 ± 0.12	2.85 ± 0.18	2.85 ± 0.06	2.32 ± 0.30**	2.78 ± 0.14	2.62 ± 0.12
A/G (ratio)	1.01 ± 0.09	1.06 ± 0.06	1.08 ± 0.08	1.17 ± 0.08*	0.95 ± 0.10	1.26 ± 0.12**
Protein fraction (%)						
Albumin	50.2 ± 2.2	51.4 ± 1.4	51.9 ± 1.8	53.8 ± 1.8*	48.5 ± 2.5	55.8 ± 2.5**
Globulin α_1	19.9 ± 3.9	19.9 ± 1.7	21.2 ± 2.3	14.3 ± 2.5*	23.7 ± 2.2	14.4 ± 2.3**
Globulin α_2	8.04 ± 0.80	7.14 ± 0.43	6.92 ± 0.40*	5.82 ± 0.86**	6.70 ± 0.20	6.60 ± 0.22
Globulin β	16.6 ± 1.9	16.3 ± 1.1	15.0 ± 0.8	16.9 ± 0.7	16.2 ± 0.8	16.4 ± 1.5
Globulin γ	5.28 ± 0.88	5.28 ± 0.96	4.92 ± 0.57	9.18 ± 2.40**	4.86 ± 0.59	6.90 ± 0.91**
AST (IU/L)	74.6 ± 11.1	83.0 ± 22.1	103.6 ± 84.8	125.4 ± 56.1	65.6 ± 12.0	69.0 ± 5.7
ALT (IU/L)	31.2 ± 3.1	34.0 ± 5.7	48.2 ± 41.0	53.2 ± 28.0	26.0 ± 6.2	28.0 ± 6.4
ALP (IU/L)	357.2 ± 28.6	366.6 ± 88.4	551.6 ± 95.2**	630.0 ± 72.0**	251.0 ± 30.2	534.4 ± 78.0**
γ-GTP (IU/L)	0.52 ± 0.25	0.60 ± 0.20	0.54 ± 0.15	2.56 ± 2.20	0.58 ± 0.19	1.08 ± 1.70
Total bilirubin (mg/dL)	0.066 ± 0.018	0.044 ± 0.011	0.052 ± 0.022	0.390 ± 0.260**	0.054 ± 0.009	0.080 ± 0.027
Glucose (mg/dL)	166.2 ± 6.9	173.2 ± 19.0	156.8 ± 3.4	122.0 ± 4.6**	180.0 ± 17.0	154.6 ± 28.0
Total cholesterol (mg/dL)	67.0 ± 9.7	44.6 ± 7.6*	40.6 ± 7.8*	53.4 ± 20.0	56.8 ± 8.6	58.2 ± 8.6
Triglycerides (mg/dL)	37.4 ± 14.3	45.2 ± 12.8	33.6 ± 12.0	27.2 ± 5.40	56.6 ± 21.7	19.0 ± 5.50**
BUN (mg/dL)	15.7 ± 0.8	15.6 ± 0.9	16.2 ± 3.5	21.9 ± 1.2**	14.9 ± 1.1	19.7 ± 2.3**
Crea (mg/dL)	0.57 ± 0.03	0.56 ± 0.03	0.54 ± 0.04	0.48 ± 0.05**	0.54 ± 0.04	0.49 ± 0.05
Na (mEq/L)	143.8 ± 0.8	143.8 ± 0.8	143.8 ± 1.3	144.4 ± 2.4	140.6 ± 0.5	140.2 ± 0.8
K (mEq/L)	4.68 ± 0.32	4.86 ± 0.28	4.98 ± 0.22	4.83 ± 0.75	4.74 ± 0.62	5.32 ± 0.38
CI (mEq/L)	109.0 ± 0.7	108.2 ± 1.1	108.8 ± 1.8	110.2 ± 0.8	103.6 ± 1.1	105.4 ± 1.7
Ca (mg/dL)	9.52 ± 0.38	9.62 ± 0.36	9.40 ± 0.32	8.38 ± 0.26**	10.0± 0.05	9.04 ± 0.37**
IP (mg/dL)	6.60 ± 0.27	7.06 ± 0.74	6.64 ± 0.74	7.28 ± 0.36	6.92 ± 0.59	8.12 ± 0.73*
FEMALES						
Number of animals examined	5	5	5	1	5	5
Total protein (g/dL)	6.20 ± 0.23	6.50 ± 0.31	6.16 ± 0.19	5.30[a]	6.20 ± 0.23	4.56 ± 0.77**
Albumin (g/dL)	2.96 ± 0.23	3.34 ± 0.25*	3.26 ± 0.13	2.38[a]	3.53 ± 0.26	2.68 ± 0.43**
A/G (ratio)	0.92 ± 0.09	1.05 ± 0.09	1.13 ± 0.08**	0.81[a]	1.32 ± 0.11	1.45 ± 0.12
Protein fraction (%)						
Albumin	47.7 ± 2.6	51.3 ± 2.2*	52.9 ± 1.7**	44.8[a]	56.9 ± 2.1	59.1 ± 1.9
Globulin α_1	19.9 ± 2.1	18.8 ± 1.6	17.6 ± 1.9	16.3[a]	15.7± 1.5	10.6 ± 3.5*
Globulin α_2	7.98 ± 0.61	6.82 ± 0.69*	7.22 ± 0.73	7.80[a]	5.72 ± 0.64	6.54 ± 1.41
Globulin β	19.0 ± 1.5	17.7± 1.6	16.9 ± 0.7	17.2[a]	14.7± 1.0	14.8 ± 2.2
Globulin γ	5.46 ± 1.30	5.32 ± 0.88	5.36 ± 0.89	13.90[a]	7.06 ± 1.60	9.00 ± 3.80
AST (IU/L)	79.4 ± 12.8	66.8 ± 4.7	87.0 ± 48.1	147.0[a]	66.2 ± 8.7	143.6 ± 104.0**
ALT (IU/L)	26.2 ± 4.0	24.4 ± 2.3	28.2 ± 6.2	32.0[a]	27.2 ± 7.5	53.4 ± 61.0
ALP (IU/L)	199.6± 21.6	180.0 ± 62.0	174.6 ± 40.7	499.0[a]	144.4± 44.7	657.4 ± 439.0**
y-GTP (IU/L)	0.62 ± 0.28	0.62 ± 0.36	0.54 ± 0.11	1.50[a]	0.50 ± 0.20	15.4 ± 17.0**
Total bilirubin (mg/dL)	0.048 ± 0.008	0.046 ± 0.009	0.038 ± 0.008	0.070[a]	0.074± 0.011	1.240 ± 2.300
Glucose (mg/dL)	145.0± 23.0	150.4 ± 8.7	160.8 ± 13.0	121.0[a]	140.4± 19.0	115.4 ± 25.0
Total cholesterol (mg/dL)	67.2 ± 19.0	55.6 ± 16.0	45.8 ± 12.0	54.0[a]	69.2 ± 15.0	55.2 ± 22.0
Triglycerides (mg/dL)	26.8 ± 8.9	67.4 ± 86.9	33.0 ± 15.2	19.0[a]	17.4 ± 4.5	21.2 ± 10.0
BUN (mg/dL)	26.52 ± 4.52	22.74 ± 3.84	23.34 ± 2.77	29.70[a]	15.98± 1.04	17.06 ± 4.14
Crea (mg/dL)	0.62 ± 0.03	0.60 ± 0.01	0.59 ± 0.03	0.48[a]	0.60 ± 0.02	0.52 ± 0.03**
Na (mEq/L)	139.0± 2.0	139.2 ± 1.9	138.2 ± 2.0	139.0[a]	140.2± 1.3	139.6 ± 0.9
K (mEq/L)	4.97 ± 0.17	5.23 ± 0.20	5.11 ± 0.28	5.44[a]	4.50 ± 0.56	4.97 ± 0.30
CI (mEq/L)	103.6± 1.3	104.4 ± 1.5	103.4 ± 1.1	106.0[a]	104.8± 0.8	104.8 ± 0.8
Ca (mg/dL)	10.5 ± 0.5	10.6 ± 0.5	10.4 ± 0.3	9.70[a]	10.3 ± 0.2	9.2 ± 0.8**
IP (mg/dL)	8.96 ± 0.71	8.42 ± 0.40	8.76 ± 0.86	7.80[a]	6.62 ± 0.51	7.82 ± 1.40

Values are given as the mean ± S.D.

*Significantly different from the control, $p \leq 0.05$.

**Significantly different from the control, $p \leq 0.01$.

[a]Data from only one animal. In this group, other females did not deliver pups normally or survive to the end of the study.

significantly increased at 0.5 and 2.5 mg/kg/day in males. Significant increases in T-Bil and BUN and decreases in glucose, Crea, and Ca were noted in the 2.5 mg/kg/day group. Furthermore, T-Cho was significantly decreased at 0.1 and 0.5 mg/kg/day in males. Significant decreases in TP, the α_1-globulin fraction ratio, TG, and Ca, and significant increases in albumin and the γ-globulin fraction ratios, ALP, BUN, and IP were observed in males of the 2.5 mg/kg/day group at the end of recovery periods.

In females in the main group, many changes, including decreases in TP, albumin, and Crea, and increases in AST, ALP, γ-GTP, and T-Bil, were found in one female in the 2.5 mg/kg/day group (Table III). The albumin fraction ratio was significantly increased in females in the 0.1 and 0.5 mg/kg/day groups. Significant decreases in TP, albumin, α_1-globulin fraction ratio, Crea, and Ca, and significant increases in AST, ALP, and γ-GTP were observed in females in the recovery group at 2.5 mg/kg/day.

Necropsy Findings

In the main group, gross observations at necropsy revealed atrophy of the thymus in 3/7 males and 10/12 females, atrophy of the spleen in 3/7 males and 5/12 females, yellowish brown discoloration of the liver in 7/7 males and 6/12 females, black patches on the glandular stomach mucosa in 4/12 females, pancreas edema in 2/12 females, small-sized epididymis in 4/7 males, small-sized seminal vesicle in 4/7 males, pale yellow discoloration of the subcutis of general skin in 1/12 females, and atrophy of the lateral great muscle in 3/7 males at 2.5 mg/kg/day. In addition, opacity of the eye ball, granular surface on the forestomach mucosa, thickening of the forestomach mucosa, diverticulum of the ileum, yellow mass of the epididymis cauda, and yellow patches on the epididymis corpus were each observed in 1 male given 2.5 mg PFDoA/kg/day. Blood retention was identified in the uterus in five of seven females that died or were euthanized due to a moribund condition at the end of the gestation period in the 2.5 mg/kg/day group.

Yellowish brown or yellow discoloration in the liver (5/5 males and 4/5 females) and enlarged liver (4/5 males and 2/5 females), atrophy of the thymus (1/5 males and 1/5 females), spleen atrophy (1/5 females), edema of the submandibular gland and sublingual gland (1/5 females), atrophy of the lateral great muscle (1 female), pale yellow discoloration of the subcutis of the general skin (1 female), and small-sized seminal vesicle (1 male) were observed in the 2.5 mg/kg/day recovery group.

Organ Weight

The relative weight of the liver in males was significantly higher at 0.5 mg/kg/day and 2.5 mg/kg/day at the end of the administration period (Table IV). The absolute and relative weights of the thymus and absolute weights of the kidney, spleen, heart, pituitary gland, thyroid, adrenal gland, and epididymis in males given 2.5 mg PFDoA/kg/day were significantly decreased while the relative weights of the kidney and brain were significantly increased.

In females in the main group, many changes, including an increase in the relative liver weight and decreases in the absolute and relative weights of the spleen and thymus, were found in one surviving female given 2.5 mg/kg/day (Table IV). A significant increase in the relative liver weight and significant decreases in absolute weights of spleen, heart, pituitary gland, and thymus were observed at the end of the administration period in females given 0.5 mg PFDoA/kg/day.

Most changes observed in males given 2.5 mg PFDoA/kg/day at the end of the administration period remained after the 14-day recovery period (Table IV). In addition, the relative weights of testes and epididymides were significantly increased in the male recovery group. Significant increases in the relative weights of the brain, liver, and kidney and significant decreases in the absolute and relative weights of the ovary and absolute weights of the heart, pituitary gland, and adrenal gland were observed in females in the 2.5 mg/kg/day recovery group.

Histopathological Findings

Upon completion of the administration period, hepatic changes were observed in all males and females given 2.5 mg PFDoA/kg/day (Table V). They included diffuse hepatocyte hypertrophy, peribiliary inflammatory cellular infiltration, single cell necrosis of hepatocytes, focal necrosis, bilirubin deposition, and bile duct proliferation. The incidence of diffuse hepatocyte hypertrophy in both sexes and single cell necrosis of hepatocytes in females was significantly higher in the 2.5 mg/kg/day group. Focal necrosis was also detected in two females given 0.5 mg PFDoA/kg/day.

Histopathological changes were observed not only in the liver, but also in various organs in the 2.5 mg/kg/day group (Table V). A reduction in zymogen granules was seen in the pancreas in both sexes, and the frequency of the reduction in males was significantly increased. The incidence of edema of the interstitium in the pancreas was significantly higher in females in the 2.5 mg/kg/day group than in the controls. Atrophic changes were observed in the spleen, thymus, adrenal gland, muscle fibers, and male reproductive organs. The incidences of adrenal cortex atrophy in males and thymus cortex atrophy in females were significantly increased. Furthermore, a decrease in hematopoiesis in the bone marrow, ulcers in the glandular stomach, and erosion, hyperkeratosis, squamous cell hyperplasia, and inflammatory cellular infiltration, edema, and fibrosis of submucosa in the forestomach were noted.

As for male reproductive organs, atrophy of the glandular epithelium was observed in the prostate, seminal vesicle, and coagulating gland (Table V). In addition, cell debris at